Division of Applied Sciences
Harvard University — Cambridge, Massachusetts

ANNUAL PROGRESS REPORT NO. 104

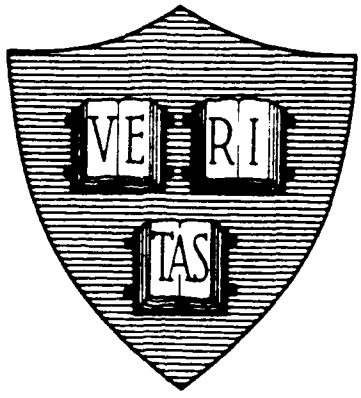

JOINT SERVICES ELECTRONICS PROGRAM
N00014-89-J-1023

Covering Period

August 1, 1989 — July 31, 1990

July 1990

REPORT DOCUMENTATION PAGE

Form Approved
OMB No 0704-0188

1a REPORT SECURITY CLASSIFICATION Unclassified	1b RESTRICTIVE MARKINGS None
2a SECURITY CLASSIFICATION AUTHORITY N/A	3 DISTRIBUTION/AVAILABILITY OF REPORT Unclassified/Unlimited
2b DECLASSIFICATION/DOWNGRADING SCHEDULE N/A	
4 PERFORMING ORGANIZATION REPORT NUMBER(S) Annual Progress Report No. 104	5 MONITORING ORGANIZATION REPORT NUMBER(S)
6a NAME OF PERFORMING ORGANIZATION Harvard University 6b OFFICE SYMBOL (If applicable) N/A	7a NAME OF MONITORING ORGANIZATION Office of Naval Research
6c ADDRESS (City, State, and ZIP Code) Division of Applied Sciences Harvard University Cambridge, MA 02138	7b ADDRESS (City, State, and ZIP Code) 800 N. Quincy Street Arlington, VA 22217
8a NAME OF FUNDING SPONSORING ORGANIZATION Office of Naval Research 8b OFFICE SYMBOL (If applicable)	9 PROCUREMENT INSTRUMENT IDENTIFICATION NUMBER N00014-89-J-1023
8c ADDRESS (City, State, and ZIP Code) 800 N. Quincy Street Arlington, VA 22217	10 SOURCE OF FUNDING NUMBERS PROGRAM ELEMENT NO / PROJECT NO / TASK NO / WORK UNIT ACCESSION NO

11 TITLE (Include Security Classification)
Annual Progress Report No. 104

12 PERSONAL AUTHOR(S)
Prof. Michael Tinkham

13a TYPE OF REPORT	13b TIME COVERED	14 DATE OF REPORT (Year, Month, Day)	15 PAGE COUNT
Technical	FROM 8/1/89 TO 7/31/90	July 31, 1990	116

16 SUPPLEMENTARY NOTATION

17 COSATI CODES			18 SUBJECT TERMS (Continue on reverse if necessary and identify by block number)
FIELD	GROUP	SUB-GROUP	

19 ABSTRACT (Continue on reverse if necessary and identify by block number)

An annual report of the JSEP (Joint Services Electronics Program) in solid state electronics, quantum electronics, information electronics, control and optimization, and electromagnetic phenomena is presented. Results of the research to date are summarized and significant accomplishments are discussed.

20 DISTRIBUTION/AVAILABILITY OF ABSTRACT ☐ UNCLASSIFIED/UNLIMITED ☐ SAME AS RPT ☐ DTIC USERS	21 ABSTRACT SECURITY CLASSIFICATION
22a NAME OF RESPONSIBLE INDIVIDUAL	22b TELEPHONE (Include Area Code) / 22c OFFICE SYMBOL

Joint Services Electronics Program

N00014-89-J-1023

ANNUAL PROGRESS REPORT NO. 104

Covering Period

August 1, 1989 — July 31, 1990

The research reported in this document, unless otherwise indicated, was made possible through support extended to the Division of Applied Sciences, Harvard University by the U. S. Army Research Office, the U. S. Air Force Office of Scientific Research and the U. S. Office of Naval Research under the Joint Services Electronics Program by Grant N00014-89-J-1023. Related research sponsored by the Office of Naval Research, the National Science Foundation, the National Aeronautic and Space Administration, and by the University is also reported briefly with appropriate acknowledgment.

Division of Applied Sciences
Harvard University
Cambridge, Massachusetts

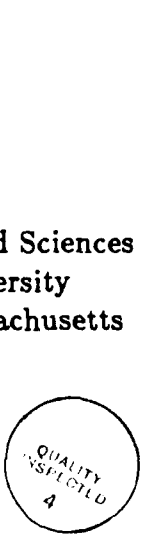

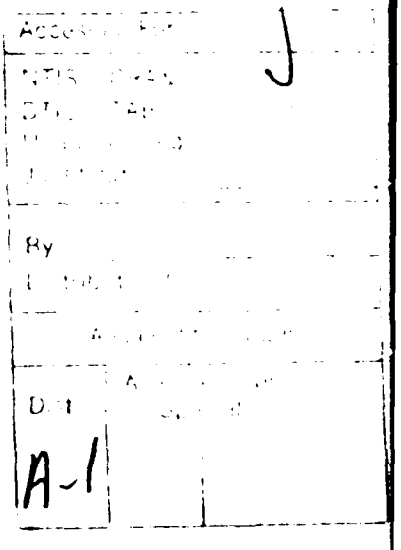

ANNUAL PROGRESS REPORT NO. 104

Joint Services Contract

N00014-89-J-1023	The Steering Committee

Related Contracts

N00014-86-K-0033	H. Ehrenreich
N00014-86-K-0760	H. Ehrenreich
N00014-87-K-0511	J. A. Golovchenko
N00014-89-J-1565	M. Tinkham
N00014-89-J-1592	R. M. Westervelt
N00014-90-J-1093	Y. C. Ho
N00014-90-J-1234	J. A. Golovchenko
NSF-CDR-88-03012	J. J. Clark, Y. C. Ho
NSF-DMR-88-12855	P. S. Pershan
NSF-DMR-88-17309	R. M. Westervelt
NSF-DMR-88-58075	E. Mazur
NSF-DMR-89-12927	M. Tinkham
NSF-DMR-89-20490	H. Ehrenreich, A. Golovchenko E. Mazur, W. Paul, P. S. Pershan, M. Tinkham, R. M. Westervelt
NSF-ECS-85-15449	Y. C. Ho
DAAL03-86-K-0171	Y. C. Ho
DAAL03-88-K-0114	E. Mazur
DAAL03-88-G-0078	E. Mazur
DAAL02-89-K-0097	T. T. Wu
DAAL03-89-G-0076	R. M. Westervelt
DE-FG02-84-ER40158	T. T. Wu
DE-FG02-88-ER45379	P. S. Pershan
DE-FG02-89-ER45399	J. A. Golovchenko
F19628-88-K-0024	T. T. Wu
AFOSR-89-0506	R. M. Westervelt

JOINT SERVICES ELECTRONICS PROGRAM

August 1, 1989 — June 30, 1990

ADMINISTRATIVE STAFF

Contracts

N00014-89-J-1023

The Steering Committee

Prof. N. Bloembergen
Assoc. Prof. J. J. Clark
Prof. H. Ehrenreich
Prof. J. A. Golovchenko
Prof. Y. C. Ho
Assoc. Prof. E. Mazur
Prof. W. Paul
Prof. P. S. Pershan
Prof. M. Tinkham
Prof. R. M. Westervelt
Prof. T. T. Wu

RESEARCH STAFF

Dr. N. Bloembergen
Dr. J. H. Burnett
Dr. J. J. Clark
Dr. H. Ehrenreich
Dr. Y. C. Ho
Dr. J. Q. Hu
Dr. P. M. Hui
Dr. N. F. Johnson
Dr. R. W. P. King
Dr. C. J. Lobb
Dr. C. Z. Lũ
Dr. C. M. Marcus
Dr. E. Mazur
Dr. J. M. Myers
Dr. W. Paul
Dr. P. S. Pershan
Dr. T. Rabedeau
Dr. M. Rzchowski
Dr. H. M. Servi
Dr. H.-M. Shen
Dr. S. Strickland
Dr. M. Tinkham
Dr. R. M. Westervelt
Dr. T. T. Wu
Dr. B. Zhang

INTRODUCTION

This report covers progress made during the past year in the work of eleven Research Units funded under the Joint Services Electronics Program at Harvard University. It is broken down into four major divisions of electronic research: *Solid state electronics, Quantum electronics, Information electronics, and Electromagnetic phenomena.* Following the report of the work of each Unit, there is a complete annual report of the associated Publications/Patents/Presentations/Honors. This report also includes a section on *Significant Accomplishments* which contains selected highlights from two of these areas. These are "Second-harmonic Efficiency and Reflectivity of GaAs During Femtosecond Melting" by Research Unit 7 and "Electromagnetic Field of a Vertical Dipole over Earth or Sea with Applications to Communication and Over-the-Horizon Radar" by Research Unit 11.

CONTENTS

V. SIGNIFICANT ACCOMPLISHMENTS REPORT

I. SOLID STATE ELECTRONICS

Personnel

Prof. H. Ehrenreich
Prof. W. Paul
Prof. P. S. Pershan
Prof. M. Tinkham
Prof. R. M. Westervelt
Prof. J. A. Golovchenko
Assoc. Prof. C. J. Lobb
Dr. J. H. Burnett
Dr. M. Iansiti
Dr. N. F. Johnson
Dr. C. M. Marcus
Dr. T. Rabedeau
Dr. M. Rzchowski
Dr. P.-M. Hui
Dr. F. R. Waugh
Mr. K. Babcock
Mr. S. P. Benz
Mr. H. Cheong
Mr. S. K. Leonard
Mr. R. Martinez
Mr. I. Tidswell
Mr. M. Young
Mr. R. Seshadri

I.1 Electronic Theory of Semiconductor Alloys and Superlattices. H. Ehrenreich, Contract N00014–89–J–1023; Research Unit 1.

During the past year the research efforts of the group have been concentrated on 1) the electronic and optical properties of III-V and II-VI superlattices, 2) the electronic structure of wide band gap superlattices containing DMS (diluted magnetic semiconductor) barrier layers, 3) excitons in superlattices, and 4) scattering effects on tunneling in double barrier quantum well structures.

A. III-V and II-VI Superlattices

A comprehensive paper summarizing the group's research concerning the electronic structure and optical properties of III-V and II-VI superlattices was published during the past year [1]. In this context additional calculations for the optical absorption in II-VI HgTe/CdTe superlattices, corresponding to samples prepared by J. Schetzina (North Carolina State University), were performed. The agreement for best

samples was sufficiently good as to be practically indistinguishable from the experimental results. For samples having particularly thin barriers or wells the agreement was far poorer, suggesting that either the superlattice formalism fails in this limit or that the quality of such samples is inherently poorer. Schetzina agrees that the latter is the more likely possibility. This conclusion is also in accord with our experience based on comparing the present theoretical calculations with those using an extended basis by T. C. McGill's group at Caltech (N. F. Johnson, H. Ehrenreich, G. T. Wu, and T. C. McGill, *Phys. Rev.* **B38**, 13095, 1988).

The superlattice representation formalism that we have developed to perform these calculations is based on a $\mathbf{k} \cdot \mathbf{p}$ approach which is optimally adapted for this purpose. The approach is attractive because it recognizes at the outset that a superlattice is a periodic structure, and that therefore the extensive formalism developed to treat crystalline solids is applicable. This approach is easily implemented by transforming at the outset to a superlattice representation, and using only parameters corresponding to the bulk constituents and empirical band offsets.

Reference:

1. N. F. Johnson, H. Ehrenreich, P. M. Hui, and P. M. Young, *Phys. Rev.* **B41**, 3655 (1990).

B. DMS Alloys and Superlattices

The effects of Mn d electrons in II-VI diluted magnetic semiconductor alloys on the band edge states has been examined. The $\mathbf{k} \cdot \mathbf{p}$ formalism has been extended to take into account d states, and the hybridization between them and s-p states. These calculations have been performed with the inclusion of spin polarization effects, which are meant to model the effects of applying an external magnetic field. The addition of a nonzero-spin polarization leads to an effective sp Hamiltonian having the same form

as that of the usual mean-field exchange Hamiltonian for DMS [1].

This formalism has been extended to apply to superlattices such as CdTe/CdMnTe and ZnCdSe/ZnMnSe. The latter superlattice has a band gap in the blue-green portion of the spectrum, and therefore has potential applications for optical information processing involving visible light. The DMS barrier layer is particularly attractive since it can be lattice matched to the nonmagnetic containing layer forming the quantum well. This feature may be sufficiently important to renew interest in DMS materials, which, for entirely understandable reasons has waned during the past few years.

Results for the above-mentioned superlattices have shown, for example, that the analysis of Nurmikko's group at Brown University (S. K. Chang *et al.*, *Phys. Rev.* **B37**, 1191, 1988) for determining band offsets using photoluminescence spectroscopy in magnetic fields can be understood on the basis of more fundamental considerations. Fortunately this analysis is largely independent of strain effects which are important in the Cd system. However, experimentally observed strain and magnetic field splittings cannot be reconciled with the same value of the valence band offset parameter, casting some doubt on the quality of the sample.

Reference:

1. P. M. Hui, H. Ehrenreich, and K. C. Hass, *Phys. Rev.* **B40**, 12346 (1989).

C. Valence Band Offset Controversy in HgTe/CdTe

While it was believed that the valence band offset controversy in this material had been resolved by this group [Johnson, Hui, and Ehrenreich, *Phys. Rev. Lett.* **61**, 1993 (1988)], a recent paper by J. B. Choi *et al.* [*Phys. Rev.* **B41**, 10872 (1990)] has once again raised the possibility that the offset is far smaller than the 350 meV inferred

from photoemission data. More extensive calculations than those performed previously indicate that this conclusion is incorrect. We have now surveyed superlattices having a variety of well and barrier widths, and have shown that in each case there is a semimetallic region separating two semiconducting regions for all physically possible band offsets. The results of Chen *et al.* are consistent with both a *small* offset (as they suggest) *and* an offset in the vicinity of 400 meV. Preference for the latter value comes from its agreement with the results of photoemission experiments.

D. Excitons

N. F. Johnson, a postdoctoral fellow with the group has formulated a nonvariational approach for calculating exciton binding energies in superlattices [1]. The approach is sufficiently versatile that it applies both to isolated quantum wells and to superlattices having strongly interacting wells. The agreement between the theoretically calculated and experimentally observed exciton binding energy lies within experimental error of the latter for a range of samples of $GaAs/Ga_{0.7}Al_{0.3}As$ having equal well and barrier widths for lattice periods extending from 25 to 200 Å.

The results of this work have also been used in analyzing the data for CdTe/CdMnTe discussed above.

Reference:

1. N. F. Johnson, *J. Phys. Condens. Matter* **2**, 2099 (1990).

E. Parabolic Quantum Wells

N. F. Johnson of this group collaborated with B. I. Halperin, L. Brey, and J. Dempsey in research involving the electronic and optical properties of parabolic quan-

tum wells which show interesting many electron effects. They have shown, for example, that an n-doped parabolic quantum well absorbs infrared radiation at the bare harmonic oscillator frequency independently of the electron-electron interaction, and the number of electrons in the well [1]. They have extended these considerations to imperfect parabolic quantum wells and finally to a superlattice embedded in a parabolic potential.

This work is principally supported by Harvard's Materials Research Laboratory, which the Principal Investigator of this unit directed for the past eight years. Johnson's considerable part in this effort was supported by JSEP and other DOD grants.

Reference:

1. L. Brey, N. F. Johnson, and B. I. Halperin, *Phys. Rev.* **B40**, 10647 (1989).

F. Tunneling in Resonant Double Barrier Quantum Well Structures

In its initial stages the research on these systems will be concerned with elastic and inelastic scattering processes during the tunneling process which causes the tunneling to be partly incoherent, thereby reducing its effectiveness. Quantum transport theory based on the Kubo formalism is being applied to address this problem. Principal results obtained thus far apply to simply models and not to realistic systems. This work will be enlarged during the coming year.

ANNUAL REPORT OF

PUBLICATIONS/PATENTS/PRESENTATIONS/HONORS

a. Papers Submitted to Refereed Journals (and not yet published)

P. M. Young and H. Ehrenreich, "Effects of d Bands on Semimagnetic Superlattice Band Structure," submitted to *Phys. Rev.* **B**.

b. Papers Published in Refereed Journals

P. M. Hui, H. Ehrenreich, and K. C. Hass, "Effects of d Bands on Semiconductor sp Hamiltonians", *Phys. Rev.* **B40**(18), 12346 (1989). (Partially supported by N00014-86-K-0760, N00014-84-K-0465, and N00014-89-J-1023)

L. Brye, N. F. Johnson, and B. I. Halperin, "Optical and Magneto-Optical Absorption in Parabolic Quantum Wells," *Phys. Rev.* **B40**, 10647 (1989)

N. F. Johnson, H. Ehrenreich, P. M. Hui, and P. M. Young, "Electronic and Optical Properties of III-V and II-VI Semiconductor Superlattices", *Phys. Rev.* **B41**(6), 3655 (1990). (Partially supported by N00014-86-K-0033, N00014-84-K-0465, and N00014-89-J-1023)

B. E. Larson and H. Ehrenreich, "Exchange in II-VI-based Magnetic Semiconductors," *J. Appl. Phys.* **67**(9), 5084 (1990). (Partially supported by N00014-86-K-0760 and DMR-8657472)

N. F. Johnson and H. Ehrenreich, "Infrared Optical Properties of III-V and II-VI Superlattices", *Surface Science* **228**, 197 (1990). (Partially supported by N00014-84-K-0465, N00014-89-J-1023, and N00014-86-K-0033)

N. F. Johnson, "Excitons in Superlattices," *J. Phys. Condens. Matter* **2**, 2099 (1990)

c. Books (and sections thereof) Submitted for Publication

Editor (with D. Turnbull), *Solid State Physics*, Vols. **44, 45** (Academic Press, 1991)

d. Books (and sections thereof) Published

Editor (with D. Turnbull), *Solid State Physics*, Vol. **43** (Academic Press, 1990)

g. Invited Presentations at Topical or Scientific/Technical Society Conferences

B. E. Larson and H. Ehrenreich, "Exchange in II-VI Based Magnetic Semiconductors," 34th Annual Conference on Magnetism and Magnetic Materials, Boston, MA, November 28–December 1, 1989

H. Ehrenreich, "Excitons, Band Offsets, and Magnetic Field Effects in III-V and II-VI Superlattices," DARPA-URI Meeting, Newport, RI, June 4–5, 1990

i. Honors/Awards/Prizes

Chairman-Elect, American Physical Society Panel on Public Affairs

j. Graduate Students and Postdoctorals Supported Under the JSEP for the Year Ending July 31, 1990

Drs. Neil F. Johnson and Pak-Ming Hui, and Mr. Paul M. Young

I.2 Pressure Dependence of Photo-Luminescence Excitation in GaAs/$Al_xGa_{1-x}As$ Multi-Quantum Wells.

J. H. Burnett, H. M. Cheong, and W. Paul, Grant N00014–89–J–1023; Research Unit 2.

We have continued our work on the properties of multi-quantum-wells and superlattices of group 3-group 5 semiconductor compounds, completing our investigation of the electronic states of GaAs/$Al_xGa_{1-x}As$ coupled double quantum wells (CDQW's). Our particular approach is to study the pressure dependence of suitable optical spectra of such structures as a way to clarify the mechanisms of quantized state formation and of tunneling between adjacent wells. The rationale for this method is the fact that the pressure dependences of the band structures of the well and barrier material are well established, and therefore a pressure experiment may be used to study the effect of varying the band structures in a known way in a single structure, without courting the difficulty of unknown parameter changes when materials of different x-value, or different dimensions, are made.

The optical techniques chosen as the most suitable for high pressure measurements of GaAs/$Al_xGa_{1-x}As$ quantum well energy levels are photoluminescence (PL) and photoluminescence excitation (PLE) spectroscopy. PLE in particular has allowed us to monitor many of the lower energy conduction band structures of the well and barrier materials, as modified by hydrostatic pressure. For $x = 0.3$, and for pressures below 40 kbar, the principal effect of pressure is to alter the nature of the barrier: the Γ minima which are lower at atmospheric pressure, become higher than the X minima for pressures greater than about 10 kbar. Since the heterostructure system has broken symmetry in the growth direction, the electronic states of the system can consist of mixtures of bulk Γ and X states, so the coupling between the wells (in a suitably-designed structure) is expected to depend on the relative energies of the barrier Γ and X states. Thus the experiments involve a detailed study of the changes in the spectra, and of the energies of the coupled states deduced from them, especially in the pressure range between 10 and 40 kbar.

The structure with the minimal coupling is the double well, and as the first phase of this project we studied a series of coupled double quantum wells (CDQW's), with barrier widths chosen to give different degrees of coupling between pairs of wells at atmospheric pressure. These have been fabricated in collaboration with E. Koteles and B. Elman of GTE Laboratories in Waltham, Massachusetts.

As described in our last report, for strongly coupled narrow CDQW's the energies of the electron states above the well minima, i.e., the confinement energies E_c, are not observably affected by the position of the X band in the barrier region until $\sim$ 20 kbar, the pressure at which the X band is near (within $\sim$ 40 meV) the energies of the confined states. For pressures near or higher in energy than this, E_c drops with pressure by an amount dependent on the parameters of the structure. Also, the coupling splitting, Δe, decreases with pressure from 0 to 40 kbar linearly, except for some nonlinear behavior in the range 20–25 kbar. These results were confirmed by a series of repeat measurements using the pressure medium, He, which we found, after an extensive survey of possible cryogenic media, to be the most completely hydrostatic at low temperatures.

These observations on the pressure dependence of the confinement energy E_c and the coupling splitting Δe can be understood qualitatively. The confined levels at atmospheric pressure are constructed primarily from Γ-symmetry bulk states. As the X band approaches the confined levels, any admixture of X symmetry states into the wavefunctions allows the wavefunction to leak more strongly between the wells and to spread out beyond the wells via the X component of the wavefunction. This lowers the confinement energy E_c and increases the coupling splitting Δe, starting at the pressure of the barrier X band crossing. The linear decrease in Δe is a result of the pressure dependence of electron effective mass.

The strength of these effects depends on the extent of Γ-X mixing, and in principle these measurements could give a quantitative measure of the mixing. This requires a

model which relates the quantum well energy levels as a function of the relative position of the bands, in terms of some measure of the mixing strength. However the calculation of this Γ-X mixing until recently was thought to be outside the range of applicability of the envelope function formalism. In December, 1989, T. Ando, S. Wakahara, and H. Akera [1] published a formal analysis of the extension of the envelope function method to include band mixing, involving a 6×6 interface matrix, the components of which they calculated using a sps^* tight-binding model. We used a simplified version of this interface matrix, first used by Pulsford *et al.* [2], with a single phenomenological parameter γ, determining the mixing strength, to analyze our pressure measurements in terms of band mixing. Though this model is only appropriate for pressures up to the Γ-X crossing (actually anti-crossing), we found this model can quantitatively fit the data for the mixing parameter γ in the range 0.2–0.3. These calculations, though preliminary, have indicated that these kinds of measurements can successfully yield quantitative information on Γ-X mixing effects in these systems. Further, comparison of the phenomenological mixing strength γ with the results of tight-binding calculations tests the reliability of the boundary conditions assumed in this model. We are now pursuing more extensive calculations along these lines.

References:

1. T. Ando, S. Wakahara, and H. Akera, *Phys. Rev.* **B40**, 11609 (1989); T. Ando and H. Akera, *Phys. Rev.* **B40**, 11619 (1989).
2. N. J. Pulsford, R. J. Nicholas, P. Dawson, K. J. Morre, G. Duggan, and C. T. B. Foxon, *Phys. Rev. Lett.* **63**, 2284 (1989).

ANNUAL REPORT OF

PUBLICATIONS/PATENTS/PRESENTATIONS/HONORS

a. Papers Submitted to Refereed Journals (and not yet published)

J. H. Burnett and H. M. Cheong "The Inert Rare Gases Xe, Ar, and He as Cryogenic Pressure Media," resubmitted after updating to *Rev. Sc. Inst.*

J. H. Burnett, H. M. Cheong, W. Paul, P. F. Hopkins, E. G. Gwinn, A. J. Rimberg, R. M. Westervelt, M. Sundaram, and A. C. Gossard, "Photoluminescence Excitation Spectroscopy of Remotely Doped Wide Parabolic GaAs/AlGaAs Quantum Wells," submitted *to Physical Review* **B**.

b. Papers Published in Refereed Journals

J. H. Burnett, H. M. Cheong, W. Paul, E. S. Koteles, and B. Elman "Modification of the Coupling of Double Quantum Wells Through Band Structure Changes Under Hydrostatic Pressure," *Superlattices and Microstructures*, **6**(2), 167 (1989)

j. Graduate Students and Postdoctorals Supported under the JSEP for the Year Ending July 31, 1990

J. H. Burnett, final Ph.D. oral passed, June 1990. Title of thesis: "Investigation of Electronic States in GaAs/AlGaAs Coupled Double Quantum Wells Under Hydrostatic Pressure," and Mr. H. Cheong

I.3 X-ray Surface Characterization. I. Tidswell, T. Rabedeau, and P. S. Pershan, Grants N00014–89–J–1023, NSF DMR–88–12855, and NSF DMR–86–14003; Research Unit 3.

The design and function of many modern electronic devices is critically dependent on the properties of surfaces. To this end major research efforts at many industrial and governmental laboratories have been directed towards developing new, and improved, techniques for characterization of solid surfaces [1, 2]. These include electron diffraction and electron microscopy, as well as newer techniques such as tunneling electron microscopy and ion beam diffraction. On the other hand, there are no comparable techniques capable of characterizing the structure of buried interfaces [6]. In addition, none of the above-mentioned techniques provide a complete description of the surface structure of solids, and other complementary techniques are needed. We have demonstrated that specular reflection of X-rays with energies in the range of 7 keV to 15 keV can be used to characterize the surface structure of simple liquids, liquid crystals, and solids, and we propose continued development of the technique and application of the technique to surface problems relevant to electronics [2–5].

In particular if θ defines the angle of incidence as measured from the grazing condition (*i.e.*, $\theta = 90°$ is normal incidence) then the ratio between the reflected intensity $R(\theta)$ and the theoretical Fresnel Reflection Law of classical optics, $R_F(\theta)$, for a sharp flat surface with no structure is given by the relation:

$$\frac{R(\theta)}{R_F(\theta)} = \left| \rho_\infty^{-1} \int dz \left\langle \frac{\partial \rho}{\partial z} \right\rangle \exp\left[-iQz\right] \right|^2$$

where ρ_∞ is the electron density far from the surface, $Q_z = (4\pi/\lambda)\sin(\theta)$ and $R_F(\theta) \approx (\theta_c/2\theta)^4$ when $\theta >> \theta_c$. For X-rays in the range of 10 keV the dielectric constant for many materials is approximately given by the form $\epsilon \approx 1 - \rho_\infty r_e \lambda^2/\pi$, and the "critical angle" $\theta_c \approx \sqrt{1-\epsilon}$ is typically of the order of 0.2° to 0.3° [11]. For a rough, or diffuse surface $\rho_\infty^{-1}\langle \partial\rho/\partial z \rangle \approx \left(\sqrt{2\pi\sigma^2}\right)^{-1/2} \exp\left(-z^2/2\sigma^2\right)$ and the decay of $R(\theta)/R_F(\theta)$ with increasing θ is reminiscent of a Debye-Waller effect;

e.g., $R(\theta)/R_F(\theta) \approx \exp(-Q_z^2\sigma^2)$. In cases where there is some sort of layering at the surface, as for liquid crystals or certain solid surfaces, there are oscillations in the z-dependence of $\rho_\infty^{-1}\langle\partial\rho/\partial z\rangle$ and the Fourier transform of these gives rise to maxima and minima in the angular, or Q_z, dependence of the specular reflectivity $R(\theta)$. The real space structure of the electron density, along the surface normal, can be derived from the Q_z dependence of the reflectivity. In addition, the diffuse scattering that is observed by tuning the spectrometer off of the specular condition can be analyzed to determine long wavelength variations in the surface structure parallel to the plane of the surface.

Atomic length structure, within the plane of the surface, can be studied with X-rays incident at angles $\theta < \theta_c$ for which the incident beam is $\sim 100\%$ reflected, and for which the X-rays only penetrate below the surface as $\sim \exp(-\kappa z)$; where $\kappa \cong (2\pi/\lambda)\sqrt{\theta_c^2 - \theta^2}$ is typically of the order of 0.02 Å^{-1}. If the detector is moved out of the plane of incidence by an angle Θ, and above the plane of the surface by an angle β, scattering is observed at a wavevector transfer with components $Q_z \cong (2\pi/\lambda)\sin\beta$ and $Q_\perp \cong (4\pi/\lambda)\cos\beta\sin\Theta$. Since the incident radiation does not penetrate distances much larger than $1/\kappa$, the $Q_\perp$ dependence of the scattering can be analyzed to determine the atomic structure parallel to the surface. From the way in which it depends on Q_z for finite $Q_\perp$, the scattering can be analyzed to give information on the way in which the in-plane surface order varies with distance along the surface normal.

Some experimental studies on surface structure at $Q_\perp = 0$ can be carried out on the Harvard Materials Research Laboratory Rotating Anodes X-ray Facility, however most of the studies must eventually be completed using the higher intensity, and other properties, of synchrotron radiation. To this end a significant fraction of our experimental program is carried out at the National Synchrotron Light Source, Brookhaven National Laboratory.

The progress in this report period is most easily described in terms of the accompanying table. The three sets of synchrotron measurements that were carried out this period at NSLS were: (i) in July, 1989 on beam line X22b, and in February and June of 1990 on beam line X20. The four separate samples listed in the accompanying table were prepared by Dr. Jose Bevk of AT&T Bell Laboratories, transferred to our portable UHV X-ray cell, and transported to NSLS for measurement. The three types of measurements that were done were (a) specular reflectivity, (b) scattering along (m, n, Q_z) bulk truncation rods $(m, n = 1, 2 \ldots)$, and (c) scattering from structure within the plane of the surface, or $(m/2, n/2, Q_z)$ truncation rods [5, 7]. The type of measurement that was done on the different samples are indicated by $(\surd)$ in the appropriate column of the following table.

#	Date	Type of Oxidation	Specular Reflectivity $[0, 0, Q_z]$	Truncation Rod $[m, n, Q_z]$	Surface Scattering $[m/2, n/2, Q_z]$
1	7/89	Dry	$\surd$		
2		Dry & Later Exposed to Air (~6 hr)	$\surd$	$\surd$	
3	2/90	Dry	$\surd$	$\surd$	$\surd$
4a	6/90	Dry & Later Annealed @ 550°C	$\surd$	$\surd$	$\surd$
4b		& Later Exposed to Air (~2 hr)	$\surd$	$\surd$	$\surd$

Figure I.1(a) illustrates the specular reflectivity results for two samples that were oxidized with dry O_2 in the AT&T UHV chamber where they were grown. The peak at $Q_z/Q_0 = 4$ rlu [1 rlu = 1.1569 Å^{-1}] is the [004] Bragg reflection from Si. Sample #3, from February 1990 was prepared and measured at room temperature. Sample #4a, from June 1990, was prepared identically to #3 however, before being measured it was annealed at approximately 550°C for two hours. The visible differences for Q_z between 1 and 2.5 are probably due to the effects of the anneal, however because there are also slight differences between samples #1 and #3, further analysis is needed before one can be certain that the differences between samples #3 and #4a are not

due to other variables. For example, the miscut between the surface and the Si lattice is somewhat larger for sample #3 than for #4. In any event, the scattering near the [004] peak is essentially identical for the two.

Subtle differences between the ratio of R/R_F, at small values of Q_z/Q_0 can be interpreted in terms of the thickness and the roughness of the Si/SiO interface(s). For example, in Figure I.1(c) we display the ratio of R/R_F in the range $0.2 \leq Q_z \leq 1.50$ for the three samples (#1, #3, and #4a) that were only exposed to dry O_2. A rough estimate of the thickness of the oxide layer is the position of the first destructive interference minimum. Sample #4a, which was annealed, has a minimum at approximately 0.6 rlu ($\sim$0.7 Å^{-1}) corresponding to a thickness of between 4 Åand 5 Å. The minima for the other two samples are at slightly larger values of Q_z/Q_0, implying that the oxide layer is thinner. More importantly, there are qualitative differences in the amplitude of the oscillations that can, with quantitative analysis, be interpreted in terms of the widths of the various interfaces. Figure I.1(b) displays R/R_F for the same small Q_z/Q_0 region for the two samples studied in July, 1989 (#1 and #2). Sample #1 was exposed to only dry O_2, but sample #2, having been prepared in exactly the same way as #1, was then exposed to ambient atmospheric conditions. The more rapid oscillations for sample #2, with a minimum at $Q/Q_0 \sim 0.3$ rlu^{-1} (0.35^{-1}), indicates a thickness, $\sim$ 10 Å for the native oxide that was formed under room temperature. Thus the first result to be obtained in this period is that the thickness of the oxide for a Si(100) face exposed to dry O_2 at room temperature is significantly thinner than the native oxide formed under ambient conditions.

The second achievement in this period was the measurement of surface scattering and bulk truncation rods from both the dry and wet oxidized Si(001) surface. Thirteen independent surface peaks, $(m/2, n/2, Q_z \cong 0)$, were identified in sample #3, and for 9 of them it was possible to make quantitatively meaningful intensity measurements. Figure I.2 illustrates some typical transverse scans through three surface peaks. For a

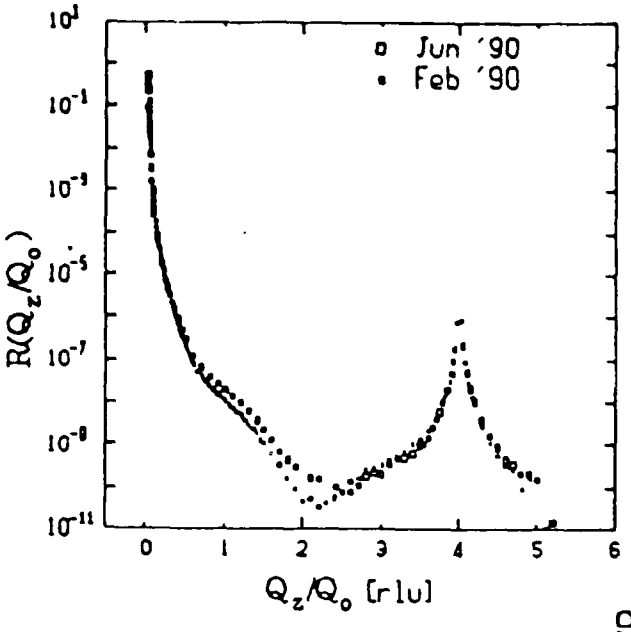

Fig. I.1a - Spec. Dry Si [001] (6/90)

Fig. I.1b - Wet vs. Dry Oxidation of Si [001] (7/89)

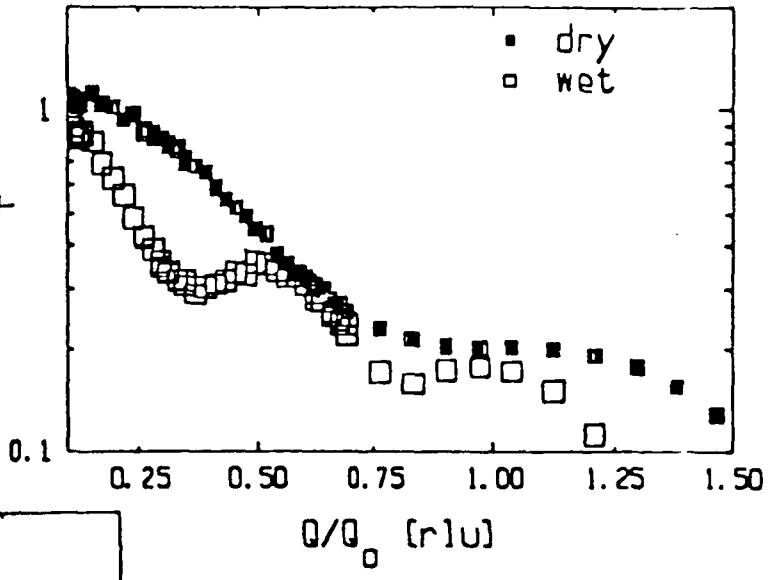

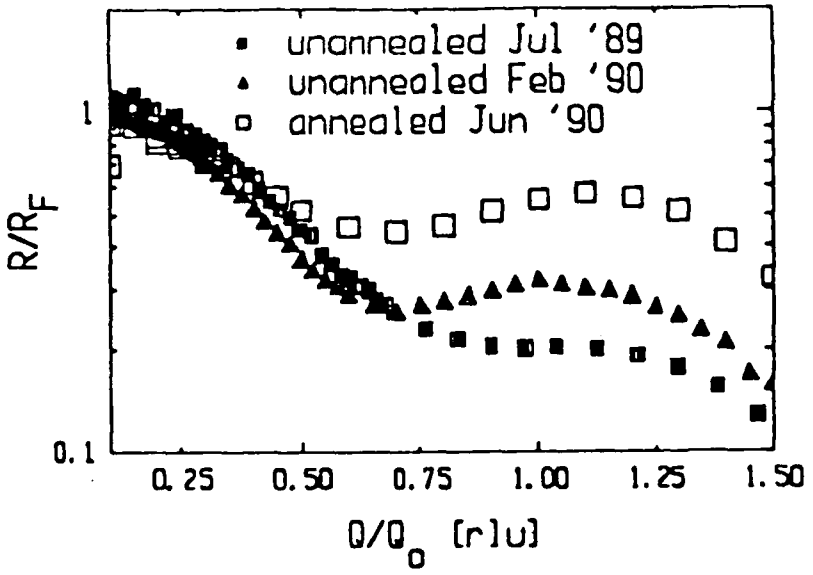

Fig. I.1c - Dry Oxidation of Si [001] (7/89)

Figure I.1. (a) Specular reflectivity from the (001) face of Si single crystals that were exposed to dry O_2: (■) exposed and measured at room temperature; (□) annealed at 550°C. The peak at $Q/Q_0 = 4$ is the (004) Bragg reflection. (b) Ratio of R/R_F for the sample exposed to only dry O_2 (■) and a similar sample that was subsequently exposed to ambient atmosphere (□). (c) The ratio of R/R_F for two samples that were exposed and measured at room temperature (■ and ▲) and the one that was annealed at 550°C).

selected subset of these, quantitative measurements were also made of the dependence of the intensity along the Q_z direction. From the analysis currently in progress it is clear that these peaks correspond to a 1×2 surface structure. RHEED data taken at AT&T on sample #4a before and after it was annealed is consistent with our observation that the intensities of the 1×2 surface peaks from sample #4a are significantly weaker than those of sample #3. On this basis we can conclude that the effect of annealing is to significantly weaken the 1×2 surface order. Interestingly, preliminary analysis of the low angle specular reflectivity data also indicates that for the annealed sample, #4a, the interface between the silicon oxide and the lattice is significantly sharper than the same interface in the unannealed samples (#1 and #3).

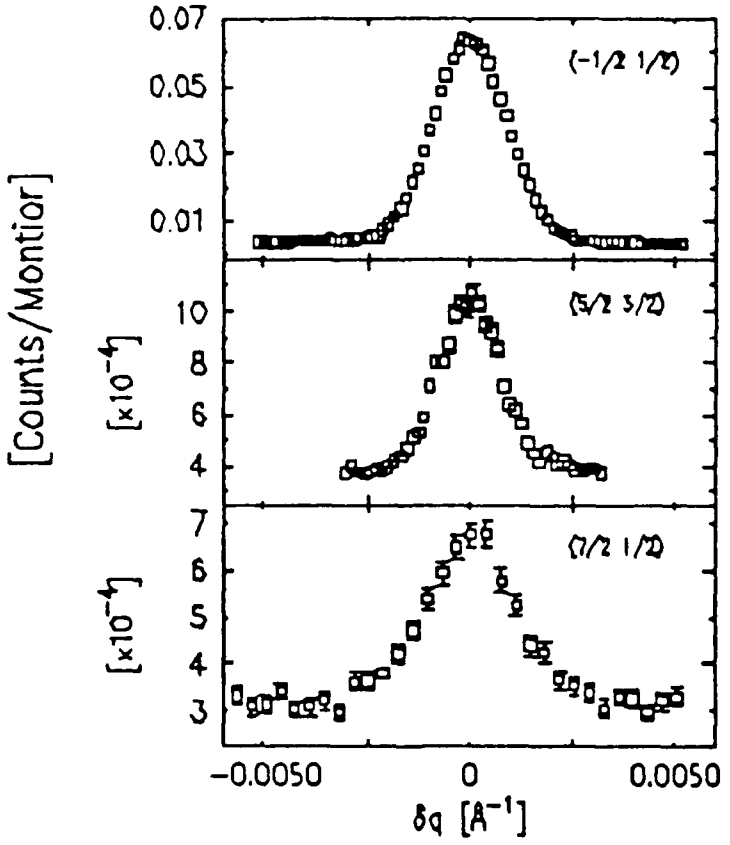

Figure I.2. Transverse scans through representative surface peaks.

Finally, we measured structure in transverse scans (i.e., along the $(1,\bar{1})$ direction) through the $(1,1,Q_z)$ truncation rods at $Q_z \sim 0.05$ rlu. Side-band structure on this can be used to characterize the long-range of surface "steps" that arise from the finite miscut between the physical surface and the [001] lattice planes.

We are currently measuring the very important buried interface between Si[001] and the SiO_2 layer, and the immediate plan is to continue systematic measurements of specular reflectivity, surface scattering, and truncation rod measurements on Si[001] under different conditions of oxidation and thermal treatment. We are in the process of analyzing data taken this spring, and for the room temperature dry oxide we hope to come up with a relatively specific model of the structure of the superficial oxide layer.

Further systems that will be studied include epitaxial Ge on Si, epitaxial Si on Ge, as well as epitaxial layers of the composition Si_xGe_{1-x} on either Si or Ge. Almost any other possible electronically interesting interface can be studied by these same techniques, and we expect to make specific choices on the basis of the most interesting technological issues and interested collaborators.

References:

1. See, for example, the collection of papers from the Symposium on Interfaces and Thin Films, *Proc. Natl. Acad. Sci. (USA)* (1987).

2. See, for example, the collection of papers from the Symposium on X-ray and Neutron Scattering from Surfaces and Thin Films, Proceedings of the International Conference on Surface and Thin Film Studies Using Glancing-incidence X-ray and Neutron Scattering, Marseille (France), *J. Physique* **50**, C–7 (1989).

3. L. Bosio, R. Cortes, A. Defrain, and M. Qumezine, *J. of Non-Cryst. Solids* **61/62**, 697 (1984).

4. R. W. James, in *The Optical Principles of the Diffraction of X-rays*, Ed. S. L. Bragg (Cornell University, Ithaca, NY, 1965).

5. P. S. Pershan, *Faraday Discuss. Chem. Soc.* **89**, to appear (1990).

6. S. A. Rice, *Nature* **316**, 108 (1985).

7. I. K. Robinson, *Phys. Rev.* **B33**, 3830 (1986).

ANNUAL REPORT OF

PUBLICATIONS/PATENTS/PRESENTATIONS/HONORS

a. Papers Submitted to Refereed Journals (and not yet published)

M. V. Baker, I. M. Tidswell, T. A. Rabedeau, P. S. Pershan, and G. W. Whitesides, "Characterization of Self-assembled Monolayers of Sulfer-containing Alkylsiloxanes on Silicon by Low Angle X-ray Reflectivity," submitted *Langmuir*, (1990). (Partially supported by NSF DMR–86–14003)

b. Papers Published in Refereed Journals

S. M. Amador and P. S. Pershan, "Light-scattering and Ellipsometry Studies of the Two-dimensional Smectic-C to Smectic-A Transition in Thin Liquid Crystal Films," *Phys. Rev.* **A 41**, 4326 (1990). (Partially supported by NSF–DMR–86–13523, and NSF–DMR–85–14003)

I. M. Tidswell, B. M. Ocko, P. S. Pershan, S. R. Wasserman, G. M. Whitesides, and J. D. Axe, "X-ray Specular Reflection Studies of Silicon Coated by Organic Monolayers (Alkylsiloxanes)," *Phys. Rev.* **B41**, 1111 (1990). (Partially supported by NSF DMR–86–14003)

S. R. Wasserman, G. M. Whitesides, I. M. Tidswell, B. M. Ocko, P. S. Pershan, and J. D. Axe, "The Structure of Self-assembled Monolayers of Alkylsiloxanes of Silicon: A Comparison of Results from Ellipsometry and Low-angle X-ray Reflectivity," *J. Am. Chem. Soc.* **111**, 5852 (1989). (Partially supported by NSF DMR–86–14003)

h. Contributed Presentations at Topical or Scientific/Technical Society Conferences

T. A. Rabedeau, I. M. Tidswell, P. S. Pershan, J. Bevk, B. S. Freer, and A. Ourmazd, "X-ray Reflectivity Studies of the Si(001)/SiO_x Interface," Materials Research Society, Boston, 1989.

j. Graduate Students and Postdoctorals Supported under the JSEP for the Year Ending July 31, 1990

Mr. Ian Tidswell and Dr. Tom Rabedeau

I.4 Superconducting Josephson Junction Arrays. S. P. Benz, M. S. Rzchowski, C. J. Lobb, and M. Tinkham, Grants N00014–89–J–1023, N00014–89–J–1565, and DMR–89–12927; Research Unit 4.

During the past year we have made much progress in measuring and interpreting the electrical properties of large (1000 × 1000) arrays of Nb-Cu-Nb thin-film SNS Josephson junctions, both at d.c. and a.c., and both with and without magnetic fluxons present. A *Phys. Rev. Letter* and a *Rapid Communication* have been published on this work, and two longer papers are in the process of being published in the *Physical Review*. The results of this work are briefly summarized here.

Our arrays serve as a model system for granular superconductors (such as the high-temperature superconductors or HTS) as well as being a system of interest in its own right. Our work on the DC properties has focussed on the closely related critical current and resistance properties, which are crucial for applications of HTS.

a) **Critical Currents**: In discussing the critical current, it is essential to distinguish between the usual practical definition in terms of a stated minimum measurable voltage criterion and an intrinsic critical current I_{co} that the array could carry (in a metastable equilibrium state) in the absence of thermally-activated fluxon motion which gives a finite resistance. In our work, we showed that I_{co} could be inferred quite reliably by taking the current value within the resistive transition at which the differential resistance dV/dI is a maximum. In zero magnetic field, this I_{co} for a 1000 × 1000 array is essentially just 1000 times that for a single junction. However, once some fluxons are inserted by a small magnetic field, the critical current is reduced by a factor typically of order 10. This occurs because an isolated fluxon feels a Lorentz force from the transport current and the energy barrier against its motion was shown by Lobb, Abraham, and Tinkham [1] to correspond to only about 10% of current that can be carried in the absence of any fluxon "defect" in the ideal lattice of the array. Of course a single moving fluxon gives a very small voltage, but for a significant flux density we

observe that a strong voltage appears at about 10% of the zero-field critical current. An interesting special case is that of "strongly commensurate fields" in which f, the average number of fluxons per unit cell in the array, takes on a value which is the ratio of two small integers, such as 1/2 or 1/3. In this case, the fluxons establish a periodic superlattice configuration (2×2 and 3×3 for these examples), which has collective pinning that is stronger that the pinning of an isolated fluxon. As a result, the critical current is higher than for a random incommensurate field value. For example, for $f = 1/2$, we showed by an exact calculation that this critical current I_{co} should be 0.414 ($= \sqrt{2} - 1$) times that in zero field, i.e., ~ 4 times greater than for an incommensurate field. Our measurements confirmed this value within experimental error, and similarly for the somewhat smaller critical current (0.268 times the zero-field value) for $f = 1/3$. In carrying out these experiments, Benz [2] mapped out in detail the differential resistance as a function of both flux density and current, providing an exceptionally well documented study.

b) Thermally Activated Resistance: The flux pinning properties discussed above in connection with critical currents also should determine the thermally activated resistance observed in the limit of small currents. We have tested this concept by a careful series of measurements of differential resistance at zero current vs. flux density and temperature. As expected from the discussion above, we found sharp cusp-like minima in resistance at the strongly commensurate field values where superlattice pinning is effective. For values of flux density f near these strongly commensurate values f_c, we find that the differential resistance rises linearly with $|f - f_c|$. For the special case of $f_c = 0$, this simply implies that the resistance arises from independently moving isolated fluxons whose number is proportional to $|f|$. The linear rise in resistance near $f_c = 1/2$ has a more subtle origin, namely isolated defects of uncertain structure moving relative to the $f = 1/2$ superlattice, or perhaps along a domain wall in the $f = 1/2$ superlattice. We have tested this interpretation in terms

of thermally-activated moving defects by plotting log R vs. $E_J(T)/kT$, where $E_J(T)$ is the independently known Josephson coupling energy of a single junction in the array. The data fall on straight lines, from whose slope we can read off the fluxon pinning energy in units of the characteristic energy $E_J(T)$. For $f \cong 0$, we find a pinning barrier in satisfactory agreement with the theoretical value 0.2 E_J predicted by Lobb *et al.* [1]. For $f \cong 1/2$, we find a somewhat larger activation energy, but we have not yet been able to make a definite assignment to the nature of the moving defect which is associated with it.

To sum up, we have developed a rather successful model for interpreting both the critical current and resistance data for a Josephson junction array in terms of "defects" in the fluxon pattern moving under the influence of the Lorentz force of the current. This work demonstrates a sort of duality rather than a difference between the Josephson junction and the flux pinning points of view used by various authors. In our work to date, we have emphasized the ideal array lattice, with only the weak (10%) intrinsic pinning. In HTS, such intrinsic pinning may be provided by the layer structure of the ideal material, because in these materials the coherence lengths are comparable with atomic dimensions. In work now underway, we plan to extend our study to include arrays with deliberately built-in imperfections that will provide extrinsic pinning of the sort which typically dominates in practical materials.

c) Giant Shapiro Steps: When we apply an a.c. current with frequency ν in the kHz to MHz range to our $N \times N$ ($N = 1000$) arrays, we find that the d.c. I-V curve displays "giant Shapiro steps" [3] at voltages equal to N times the step voltage $h\nu/2e$ for a single Josephson junction driven at the same frequency. Although the regularity of these data are evidence for the high perfection of our arrays, such effects are not new. What we have observed that *is* new and unexpected is that application of a strongly commensurate d.c. magnetic field $f = p/q$ (such as $f = 1/2$ or $1/3$, as discussed above) causes the appearance of *fractional* giant Shapiro steps at voltages that are multiples

of $(N/q)h\nu/2e$. Qualitatively, it is plausible that these fractional giant Shapiro steps result from systematic motion of the $q \times q$ vortex superlattice across the array in synchronism with the a.c. driving current. We have confirmed this interpretation by means of detailed simulations [4] which follow the time evolution of the phase differences across the various Josephson junctions in the array. All these experimental demonstrations of *coherent* time dependence across these large 2-dimensional arrays is evidence in favor of possible applications of arrays as efficient generators and detectors of electromagnetic waves.

References:

1. C. J. Lobb, D. W. Abraham, and M. Tinkham, *Phys. Rev.* **B27**, 150 (1983)
2. S. P. Benz, M. S. Rzchowski, M. Tinkham, and C. J. Lobb, *Phys. Rev.* **B**, submitted.
3. S. P. Benz, M. S. Rzchowski, M. Tinkham, and C. J. Lobb, *Phys. Rev. Lett.* **64**, 693 (1990).
4. J. U. Free, S. P. Benz, M. S. Rzchowski, M. Tinkham, C. J. Lobb and M. Octavio, *Phys. Rev.* **B41**, 7267 (1990).

I.5 High-Frequency Properties of High-Temperature Superconductors.

L. Ji, M. S. Rzchowski, and M. Tinkham,

Grants N00014–89–J–1023, N00014–89–J–1565, DMR–89–12927, and DMR–89–20490; Research Unit 4.

In previously reported work [1], we have developed a model based on Bean's critical state concept, which gives an excellent explanation of a large body of data on the generation of harmonics in the magnetization $M(t)$ when a HTS sample is immersed in an a.c. magnetic field. This work is based on a quasi-static analysis of the hysteretic response of such a sample to an a.c. magnetic field. In the past year, we have started a different type of experiment, in which HTS samples are introduced into a microwave cavity, and the dependence of the microwave loss on external parameters is determined from the change in the cavity reflection coefficient and resonant width. Because microwave frequencies exceed the characteristic frequency at which fluxon mo-

tion becomes dominated by viscous drag rather than by the pinning which dominates low frequency phenomena, the microwave loss measurements are interpreted in terms of the electrical "viscosity" of the local medium in which a given fluxon is located, rather than pinning.

Our initial round of experiments of bulk polycrystalline pellet YBCO has already revealed some unexpected results for the microwave loss after various cycles of the applied d.c. magnetic field. For example, in one experiment we compare microwave loss in a field-cooled (FC) sample [which has been cooled down through T_c in a given magnetic field H, which is then removed], and a zero-field-cooled (ZFC) sample [which has been cooled in zero field, the field H applied and then removed]. It is well known that the remanent flux density is greater in the FC case because the fluxons are pinned inside the grains when the material goes superconducting. To our surprise, we find that the microwave loss is greater *in the ZFC case*, despite its *lower* flux density. We account for this by reasoning that the ZFC sample has a greater number of fluxons in the intergranular region *between* the grains, where their viscosity is less, and hence the loss is greater. Another experimental observation that we think has not been made before is the logarithmic time dependence of the microwave loss as the fluxons "creep" out of the grains and escape. [A (log t) dependence has of course been observed in d.c. experiments using SQUIDs to measure the bulk magnetization. As noted above, however, the microwave loss measures a different aspect of the flux that is present.] This is a very small effect, but our sensitivity is high enough to pick it up, and in fact to determine a characteristic activation energy $\sim$ 1000K from the logarithmic slope.

In the near future we plan to extend these measurements to a broad frequency range by use of a strip-line geometry. This will allow us to test the theoretical frequency-dependent crossover from pinning-dominated to viscosity-dominated microwave loss. We are also beginning measurements in which the bulk HTS sample is replaced by a thin film sample of YBCO or by one of our 1000 $\times$ 1000 Josephson

junction arrays. The latter appear to give results quite similar to the granular bulk material, as might be expected from the modeling discussed earlier, but we have not yet been able to observe flux creep processes because the absolute loss levels are much lower in the arrays. Clearly, a large variety of extensions of this work lie before us, as we gain experience with our techniques and obtain higher quality, state-of-the-art samples to study.

Reference:

1. L. Ji, R. H. Sohn, G. C. Spalding, C. J. Lobb, and M. Tinkham, *Phys. Rev.* **B40**, 113370 (1989).

ANNUAL REPORT OF

PUBLICATIONS/PATENTS/PRESENTATIONS/HONORS

a. Papers Submitted to Refereed Journals (and not yet published)

M. S. Rzchowski, S. P. Benz, M. Tinkham, and C. J. Lobb, "Vortex Pinning in Josephson Junction Arrays," *Phys. Rev.* **B**, submitted. (Partially supported by NSF DMR–86–14003, DMR–89–12927, and N0014–89–J–1565)

S. P. Benz, M. S. Rzchowski, M. Tinkham, and C. J. Lobb, "Critical Currents in Frustrated Two-dimensional Josephson Arrays," *Phys. Rev.* **B**, submitted. (Partially supported by N00014–89–J–1565, DMR–89–20490, and DMR–89–12927)

A. T. Johnson, C. J. Lobb, and M. Tinkham, "Effects of Leads Upon the Retrapping Current of Josephson Junctions," *Phys. Rev. Lett.*, submitted. (Partially supported by NSF DMR–89–12927, and N00014–89–J–1565)

L. Ji, M. S. Rzchowski, and M. Tinkham, "Microwave Surface Resistance and Vortices in High-T_c Superconductors: Observation of Flux Pinning and Flux Creep," *Phys. Rev.* **B**, submitted. (Partially supported by N00014–89–J–1565, DMR–89–12927, and DMR–86–14003)

b. Papers Published in Refereed Journals

Qing Hu and M. Tinkham, "Power Spectra of Noise-induced Hopping Between Two Overlapping Josephson Steps," *Phys. Rev.* **B39**, 11358–11363 (1989). (Partially supported by ONR N00014–83–K–0383)

L. Ji, R. H. Sohn, G. C. Spalding, C. J. Lobb, and M. Tinkham "Critical State Model for Harmonic Generation in High-temperature Superconductors," *Phys. Rev.* **B40**, 10937–10945 (1989). (Partially supported by N00014–89–J–1565, NSF DMR–86–14003, and DMR–84–04489)

M. Iansiti, A. T. Johnson, C. J. Lobb, and M. Tinkham, "Quantum Tunneling and Low-voltage Resistance in Small Superconducting Tunnel Junctions," *Phys. Rev.* **B40**, 11370–11373 (1989). (Partially supported by NSF DMR–84–04489, and DMR–89–1565)

S. P. Benz, M. S. Rzchowski, M. Tinkham, and C. J. Lobb, "Fractional Giant Shapiro Steps and Spatially-correlated Phase Motion in 2D Josephson Arrays," *Phys. Rev. Lett.* **64**, 693–696 (1990). (Partially supported by NSF N00014–89–J–1565, DMR–86–14003, and DMR–89–12927)

J. U. Free, S. P. Benz, M. Rzchowski, M. Tinkham, C. J. Lobb and M. Octavio, "Dynamical Simulations of Fractional Giant Shapiro Steps in 2D Josephson Arrays," *Phys. Rev.* **B41**, 7267–7269 (1990). (Partially supported by N00014–89–J–1565, DMR–86–14003, and DMR–89–12927)

d. Books (and sections thereof) Published

M. Tinkham, "Flux Motion in High-temperature Superconductors," Article in *Physics News in 1989*, Amer. Inst. of Physics.

g. Invited Presentations at Topical or Scientific/Technical Society Conferences

M. Tinkham, "Flux Motion and Dissipation in Superconductors," Invited Lecture at Symposium on *Recent Advances in Low Temperature Physics*, Karlsruhe, W. Germany, November, 1989.

M. Tinkham, "Considerations Limiting Zero-resistance Currents in High-Temperature Superconductors," Invited Paper, MRS Fall Meeting, Boston, MA, November, 1989.

h. Contributed Presentations at Topical or Scientific/Technical Society Conferences

S. P. Benz, M. S. Rzchowski, M. Tinkham, and C. J. Lobb, "Giant Shapiro Steps and Spatially-correlated Phase Motion in 2D Josephson Arrays," March 1990 Meeting of the American Physical Society.

J. U. Free, S. P. Benz, M. Rzchowski, C. J. Lobb, and M. Tinkham, "Computer Simulations of Giant Shapiro Steps in 2D Josephson Arrays," March 1990 Meeting of the American Physical Society.

T. S. Tighe, A. T. Johnson, D. B. Ephron, C. J. Lobb, and M. Tinkham, "Electrical Characteristics of 2D Josephson Arrays," March 1990 Meeting of the American Physical Society.

S. P. Benz, M. S. Rzchowski, M. Tinkham, and C. J. Lobb, "Fractional Giant Shapiro Steps in 2D Josephson Arrays," submitted to LT19 Conference.

G. O. Zimmerman, C. J. Lobb, and M. S. Rzchowski, "Effects of Boundaries in an Array of Superconducting Weak Links," submitted to LT19 Conference.

j. Graduate Students and Postdoctorals Supported under the JSEP for the Year Ending July 31, 1990

Dr. M. Rzchowski, and Mr. S. P. Benz.

(Note: Five other students share JSEP facilities, but have no JSEP salary.)

I.6 Stability and Dynamics of Neural Networks. C. M. Marcus, F. R. Waugh, and R. M. Westervelt, Contract N00014-89-J-1025; Research Unit 5.

The hope that neural networks will provide fast, approximate solutions to computationally complex problems in real time depends critically on developing network architectures that are robust, stable, and can be implemented in parallel. We have continued and completed several studies of nonlinear dynamics in large parallel systems, focussing particular attention on analog neural networks. The thrust of the effort has been to characterize how the details of the input-output response of the individual neurons affects the collective dynamics of the network as a whole. This work has lead in the past year to the publication of three papers in *Physical Review* **A**, a *Physical Review Letter*, and the completion of a Ph.D. dissertation.

Analog neural networks are composed of processing elements with smooth, continuous input-output transfer functions. The smooth neuron transfer function distinguishes these models from the more commonly studied binary network models, in which neurons behave like Ising spins in the Ising model of magnetism. Besides providing a realistic description of analog electronic networks implemented in VLSI (as designed by Carver Mead and others), the analog models we have studied possess important computational advantages over networks of binary neurons, including the ability to be clocked in parallel with guaranteed stability against oscillation.

The stability guarantee was proven using global stability analysis and applies to networks with symmetric connections. The analysis provides a simple stability criterion which limits the gain (maximum slope) of the neuron transfer function. The result has also been generalized to include neurons with dynamic rules based on many previous states, and has been applied to analog networks configured as associative memories. Results for two standard associative memories, the Hebb rule, and the pseudoinverse rule have been presented as phase diagrams in the plane of neuron gain and the ratio of the number of stored patterns to the number of neurons. Extensive

numerical simulations have also been performed, and are found to be in agreement with analytical results.

As reported in a recent *Physical Review Letter*, we have calculated the number of fixed point attractors in an analog associative memory using techniques adapted from spin glass theory. This calculation, and supporting numerics, show that lowering neuron gain greatly reduces the number of local minima in the networks energy landscape. This result has important consequences: by using analog neurons rather than binary neurons one can achieve many of the beneficial effects of stochastic annealing. Because this type of "analog annealing" is deterministic — with neuron gain playing the role of the inverse temperature in a Monte Carlo annealing scheme — it can be easily implemented in electronic hardware without requiring special noise-generating circuitry.

The analytical techniques we have used are quite general, and can be applied to a variety of problems, particularly in artificial vision. This research is currently being carried out by Fred Waugh, a JSEP Graduate Fellow, with support from JSEP.

I.7 The Dynamics of Magnetic Domain Patterns. K. L. Babcock, R. Seshadri, and R. M. Westervelt, Contract N00014-89-J-1023; Research Unit 5.

In the past year Ken Babcock completed a systematic study of the dynamics of cellular magnetic domains in thin magnetic garnets, which has been published in a series of papers including two *Physical Review Letters*, and has resulted in invited talks for Babcock at the March Meeting of the American Physical Society and for Professor Westervelt at the Joint Soviet-American Conference on Chaos in Woods Hole, and at the Woodward Symposium in San Jose. Babcock has graduated and moved on to a postdoctoral associate in Professor Guenther Ahler's group at the University of California at Santa Barbara. Work on domain dynamics is being continued in the Westervelt group at Harvard by Raj Seshadri with JSEP support.

Cellular magnetic domains in garnet films are an example of a spatially extended system which is prevented from reaching equilibrium by topological constraints. This general problem is important for annealing of the grain structure in polycrystalline metals and the evolution of froths of soap or other materials. Similar considerations may also prove to be important in densely written magnetic recording materials. During the past year we have completed a study of the evolution of both ordered and disordered arrays of cellular domains under circumstances where the equilibrium state of the magnetic film is a single domain. The domain structure is visualized using the rotation of polarized light and analyzed using computer image processing techniques. In the high-stress regime in which the entire pattern is metastable, we have discovered interesting types of collective motion of large groups of cells: 1) ordered hexagonal arrays "melt" into disordered materials, and 2) disordered patterns composed of cellular domains with different numbers of sides respond to small increases in magnetic field with avalanches of cell destruction which involve up to 100 cells and propagate long distances. The latter result is perhaps an example of the concept of "self-organized criticality" proposed by Bak and others. The most important qualitative feature of both phenomena is that metastable domain structures can respond to small changes in conditions via large collective motions involving many cells, rather than uncorrelated single cell events. The coupling of domains in very densely written magnetic storage material could lead to similar collective events with undesirable consequences.

I.8 The Collective Behavior of Switching Charge-Density Wave Systems. S. H. Strogatz, C. M. Marcus, and R. M. Westervelt, Contract N00014–89–J–1023; Research Unit 5.

Charge density waves (CDWs) are an elegant and well-studied example of collective behavior in electronic systems. As with superconductivity, a CDW can be characterized by a single order parameter, indicating that a large number of electrons over a macroscopic size scale have condensed into a single ordered state. In the pres-

ence of an applied voltage exceeding a certain threshold, the CDW will collectively depin from impurities in the material and carry current. Usually, the transition from the pinned CDW state to the current-carrying, or sliding, state is continuous. However, in certain CDW systems, where pinning is very strong, the transition to a sliding state is found to occur in a discontinuous and hysteretic "switch." Such systems are referred to as switching samples. There is strong evidence that switching is intimately related to phase slip taking place at the pinning sites. Several years ago, Zettl and Grüner discovered experimentally a remarkable property of switching samples. They found that when the applied voltage exceeds the threshold by a small amount, the depinning transition is not immediate, but occurs after a delay. The length of the delay was also found to increase dramatically as the threshold was approached from above, ranging over several orders of magnitude.

In the past year, an analytical and numerical investigation of delayed switching in CDWs was completed by Steven Strogatz, a visiting Postdoctoral Fellow, and Charles Marcus. This research, which was published as two *Physical Review* articles, investigates the dependence of switching delay on the amount by which the depinning threshold is exceeded. The analysis was carried out for a mean-field model of the CDWs with phase-slip proposed by Strogatz, Marcus, Mirollo, and Westervelt, as well as for other models of switching CDWs in the literature. The analysis gave predictions which allow the various models to be distinguished experimentally. We note that very recent experiments on switching samples performed by M. S. Sherwin at University of California at Santa Barbara have yielded results which do not seem to correspond to any of the models of switching that have been proposed. These experiments also reveal a wealth of new phenomena that have not been accounted for theoretically.

The competition between pinning, elasticity and phase slip seen in switching CDWs is likely to be important for understanding the collective dynamics of other extended nonlinear systems with many degrees of freedom, including flux flow in type-

II superconductors and recently proposed models of earthquakes.

Steven Strogatz is currently an Assistant Professor of Applied Mathematics at MIT.

ANNUAL REPORT OF

PUBLICATIONS/PATENTS/PRESENTATIONS/HONORS

a. Papers Submitted to Refereed Journals (and not yet published)

C. M. Marcus and R. M. Westervelt, "Stability and Convergence of Analog Neural Networks with Multiple Time Step Parallel Dynamics," *Phys. Rev.* **A41**, to appear Aug. 15. (Partially supported by N00014-89-J-1592)

K. L. Babcock and R. M. Westervelt, "Dynamics of Cellular Magnetic Domain Patterns," in *Nonlinear Structures in Physical Systems*, eds. L. Lam and H. C. Morris (Springer, New York, 1990), in press. (Partially supported by N00014-89-J-1592)

R. M. Westervelt and K. L. Babcock, "Cellular Domain Patterns in Magnetic Garnet Films," in *Proc. Joint Soviet American Conference on Chaos, Woods Hole, 1989* (American Institute of Physics, New York), in press. (Partially supported by N00014-89-J-1592)

b. Papers Published in Refereed Journals

K. L. Babcock and R. M. Westervelt, "Topological 'Melting' of Cellular Domain Lattices in Magnetic Garnet Films," *Phys. Rev. Lett.* **63**, 175-178 (1989). (Partially supported by N00014-89-J-1592)

S. H. Strogatz, C. M. Marcus, R. M. Westervelt, and R. E. Mirollo, "Collective Dynamics of Coupled Oscillators with Random Pinning," *Physica* **D36**, 23-50 (1989). (Partially supported by N00014-89-J-1592)

C. M. Marcus and R. M. Westervelt, "Dynamics of Iterated-map Neural Networks," *Phys. Rev.* **A40**, 501-504 (1989). (Partially supported by N00014-89-J-1592)

K. L. Babcock and R. M. Westervelt, "Elements of Cellular Domain Patterns in Magnetic Garnet Films," *Phys. Rev.* **A40**, 2022-2037 (1989). (Partially supported by N00014-89-J-1592)

C. M. Marcus, S. H. Strogatz, and R. M. Westervelt, "Delayed Switching in a Phase-slip Model of Charge-density-wave Transport," *Phys. Rev.* **B40**, 5588-5592 (1989). (Partially supported by N00014-89-J-1592)

S. H. Strogatz and R. M. Westervelt, "Predicted Power Laws for Delayed Switching of Charge-density Waves," *Phys. Rev.* **B40**, 10501-10508 (1989). (Partially supported by N00014-89-J-1592)

K. L. Babcock, R. Seshardri, and R. M. Westervelt, "Coarsening of Cellular Domain Patterns in Magnetic Garnet Films," *Phys. Rev.* **A41**, 1952–1962 (1990). (Partially supported by N00014–89–J–1592)

C. M. Marcus, F. R. Waugh, and R. M. Westervelt, "Associative Memory in an Analog Iterated-map Neural Network," *Phys. Rev.* **A41**, 3355–3364 (1990). (Partially supported by N00014–89–J–1592)

F. R. Waugh, C. M. Marcus, and R. M. Westervelt, "Fixed-point Attractors in Analog Neural Computation," *Phys. Rev. Lett.* **64**, 1986–1989 (1990). (Partially supported by N00014–89–J–1592)

K. L. Babcock and R. M. Westervelt, "Avalanches and Self-organization in Cellular Magnetic-domain Patterns," *Phys. Rev. Lett.* **64**, 2168–2171 (1990). (Partially supported by N00014–89–J–1592)

g. Invited Presentations at Topical or Scientific/Technical Society Conferences

R. M. Westervelt, "Nonlinear Networks," *Soviet-American Conference on Chaos*, Woods Hole, Massachusetts, July 1989.

R. M. Westervelt and K. L. Babcock, "Dynamics of Cellular Magnetic Domain Patterns," in *Proc. Joint Soviet-American Conference on Chaos*, Woods Hole, Massachusetts, July 1989 (American Institute of Physics)

R. M. Westervelt, "Cellular Magnetic Domain Patterns," Nonlinear Structures in Physical Systems – Pattern Formation, Chaos, and Waves, San Jose, November 1989.

R. M. Westervelt, "Dynamics of Cellular Magnetic Domain Patterns," Dynamics Days Texas 1990, Austin, Texas, January 1990.

R. M. Westervelt, "Advantages of Analog Computation," Neural Networks for Computing, Snowbird, Utah, April 1990.

R. M. Westervelt, "Dynamics and Stability of Neural Networks," S.I.A.M. Dynamical Systems, Orlando, Florida, May 1990.

K. L. Babcock, "Coarsening, Melting, and Avalanches in Cellular Magnetic Domain Patterns," March Meeting of the American Physical Society, Anaheim, California, March 1990.

h. Contributed Presentations at Topical or Scientific/Technical Society Conferences

C. M. Marcus "Dynamics of Analog Neural Networks," *Stat. Phys.* **17**, Rio de Janeiro, Brazil, July 1989.

C. M. Marcus "Dynamics of Analog Neural Networks," Conference on Spin Glasses and Neural Networks, Porto Alegre, Brazil, August 1989.

C. M. Marcus and R. M. Westervelt, "Dynamics of Analog Neural Networks with Time Delay," *Advances in Neural Information Processing Systems* (Morgan Kauffman, San Mateo CA, 1989).

F. R. Waugh, C. M. Marcus, and R. M. Westervelt, "Nonlinear Dynamics of Analog Associative Memory Neural Networks," in *Proceedings of the International Joint Conference on Neural Networks*, Washington D.C., January 1990, Vol. I (Lawrence Erlbaum Assoc., Hillsdale, NJ, 1990), p. 321. (Partially supported by N00014-89-J-1592)

i. Honors/Awards/Prizes

C. M. Marcus, IBM Postdoctoral Fellowship.

F. R. Waugh, JSEP Graduate Fellowship.

j. Graduate Students and Postdoctorals Supported Under the JSEP for the Year Ending July 31, 1990

Dr. C. M. Marcus, Messrs. K. L. Babcock, F. R. Waugh, and R. Seshadri.

I.9 Structural and Electronic Studies of Semiconductor Interfaces and Surfaces

J. A. Golovchenko, Grant N00014-89-J-1023, Contracts N00014-87-K-0511, and NSF-DMR86-14003; Research Unit 6.

Our last report on this unit stressed several surface and interface studies on which we can now report significant progress and accomplishment. First to be described is our demonstration of an electronic device, a tunnel diode, of atomic dimensions capable of amplification and switching. Secondly, our recent success in measuring the forces between atoms on a crystal surface is presented and related to the problems of crystal epitaxy. Finally currently ongoing work on crystal epitaxy is described.

Last year's report contained a detailed description of our fundamental studies of the boron doped silicon surface using tunneling microscopy and other related diagnostic surface physics tools. This discussion focussed on structural questions and the rather unique atomic positions boron atoms occupy on silicon relative to the rest of the third column element that have been studied until now [1]. Our subsequent studies of this system dealt with the electronic consequences of this unique behavior.

The tunneling microscope is ideally suited to the study of electronic structure on an atomic scale. This electronic structure is reflected directly in the current versus voltage curves that characterize the tunnel junction formed by the tunneling tip and sample surface under investigation. The derivative or so-called dI/dV curves are widely interpreted as measuring the density of states at energy eV from the sample fermi level. Our measurements of the boron doped silicon surfaces showed regions (both in energy and coordinate space) where this differential conductivity became negative. Not only is this a direct illustration of the dangers of overly simplified interpretation often applied to tunneling microscope spectra of semiconductors (by definition, electronic density of states cannot be negative) but it also was a graphic illustration of the possibility of fashioning atomic structures having desirable characteristics of electronic devices with which we are familiar on a much larger length scale.

The regions of negative differential conductivity we discovered and identified [2, 3] displayed the electronic characteristics of the tunnel diode structure constructed several decades ago by Esaki using highly degenerately doped, diffused junction diode structures. Our structure, capable of operation in the nano-ampere regime occupies only a few square angstroms of space on the sample surface and depends solely on isolated interface states for its electrical characteristics.

We believe that this demonstration of an atomic scale device, though hardly practical for applications today, is a harbinger of the future possibilities for miniaturization to the atomic scale utilizing experience and knowledge gained from the field of surface physics. We are continuing these studies with a radically newly designed tunneling microscope and we hope to soon demonstrate extremely small three terminal devices.

On a second front, using JSEP support, we have made a fundamental advance in our ability to understand and probe crystal surfaces. In particular we can now directly measure the forces between atoms on a crystal surface using delicate light beam deflection measurements on very thin samples [4]. The sample is prepared in an ultra-high vacuum environment and doped with monolayer and submonolayer coverages of impurity atoms on one side of the sample. Their interactions result in a slight bending in the sample which can be detected with a sensitive laser beam deflection apparatus. One extracts directly the surface stress difference between the reference undoped surface on the back of the sample and the side that has been doped.

In these first measurements of this effect we have been able to make quantitative comparisons with calculations for gallium doped and clean 7×7 reconstructed surfaces showing that current theory is capable of qualitatively predicting the magnitude of stress generated at these ideal interfaces. We plan to extend these studies both to other monolayer cases and to epitaxy of strained layer systems.

Our program to study crystal epitaxy on the Harvard Tandem Ion Accelerator has now advanced to the stage where we have observed high quality (at least by channeling criteria) epitaxial silicon and germanium crystal growth on ultra-high vacuum prepared surfaces and we have been able to detect the role that metal layers on the surface can play in the growth process. This study, part of our general interest in developing the VLS (vapor liquid-metal solid semiconductor) epitaxy technique as a planar technology, shows that surface doping silicon and germanium with just a few monolayers of a metal like gold can result in enhanced growth of subsequent semiconductor epitaxial layers at reduced temperatures. It is well-known that the thick metallic layers used in the VLS process tend to "ball up" and thereby frustrate attempts to use the process for patterning areas of growth. Our preliminary studies have shown that enhanced growth may be observed at metal layer thicknesses of a few monolayers where balling up does not occur. Our preliminary results are currently being studied, extended, and articulated to establish the entire range over which this new regime of VLS may be useful for crystal growth.

We have also been studying the hetero-epitaxial growth of germanium on silicon substrates in our ultra-high vacuum tunneling microscope. We have observed Stransky Krastinov type growth with strong islanding occurring after a few monolayers of germanium deposition. The islands are faceted as expected for 111 growth directions and we are currently attempting to measure the lattice constant of the overlayer as a function of island thickness with the tunneling microscope. We are also hoping to detect the first signs of the appearance of misfit dislocations as the germanium layers are added.

References:

1. P. Bedrossian, R. D. Meade, K. Mortensen, D. M. Chen, J. A. Golovchenko, and D. Vanderbilt, *Phys. Rev. Lett.* **63**, 1257 (1990).

2. P. Bedrossian, D. M. Chen, K. Mortensen, and J. A. Golovchenko, *Nature* **342**, 258 (1989).

3. P. Bedrossian, K. Mortensen, D. M. Chen, and J. A. Golovchenko, *Nucl. Instrum. and Meth. in Phys. Res.* **B48**, 296 (1990).

3. R. E. Martinez, W.A. Augustyniak, and J. A. Golovchenko, *Phys. Rev. Lett.* **64**, 1035 (1990).

ANNUAL REPORT OF

PUBLICATIONS/PATENTS/PRESENTATIONS/HONORS

b. Papers Published in Refereed Journals

P. Bedrossian, D. M. Chen, K. Mortensen, and J. A. Golovchenko, "Demonstration of the Tunnel-diode Effect on an Atomic Scale," *Nature* **32**, 258–260 (1989). (Partial Support by NSF DMR–86–14003)

R. E. Martinez, W. A. Augustyniak, and J. A. Golovchenko, "Direct Measurement of Crystal Surface Stress," *Phys. Rev. Lett.* **64**, 1035–1038 (1990). (Partial Support by NSF DMR–86–14003)

g. Invited Presentations at Topical or Scientific/Technical Society Conferences

J. A. Golovchenko, "Structural and Electronic Studies of Semiconductor Surfaces," Physics and Chemistry of Surfaces and Interfaces Conference, Clearwater, Florida, January 29 – February 2, 1990.

h. Contributed Presentations at Topical or Scientific/Technical Society Conferences

R. E. Martinez, "Direct Measurement of Crystal Surface Stress," American Physical Society 1990 March Meeting, Anaheim, California, March 12–16, 1990. (Partial Support by NSF DMR–86–14003)

j. Graduate Students and Postdoctorals Supported under the JSEP for the Year Ending July 31, 1990

Ms. S. K. Leonard and Mr. R. E. Martinez

II. QUANTUM ELECTRONICS

Personnel

Prof. N. Bloembergen
Prof. E. Mazur
Dr. C. Z. Lü
Mr. K. H. Chen
Mr. D. S. Chung
Mr. S. Deliwala
Mr. J. Goldman
Ms. K. Y. Lee
Mr. P. Saeta
Mr. Y. Siegal
Mr. J. K. Wang

II.1 Ultrashort Laser Interactions with Semiconductor Surfaces.

N. Bloembergen, E. Mazur, P. Saeta, Y. Siegal, and J. K. Wang, Contract N00014–89–J–1023 and NSF DMR-8858075; Research Unit 7.

In this research unit the electronic and material properties of semiconductors and metals are studied using ultrashort laser pulses. Because of the small penetration depth of the laser light in such materials, and because thermal diffusion is negligible for times shorter than ten picoseconds, subpicosecond laser irradiation concentrates the laser pulse energy in a very thin layer at the surface of the material. At high pulse energies the melting threshold can thus easily be reached, and the material at the surface can transform into short-lived phases that can sometimes not be obtained by any other method. At pulse energies below the melting threshold, measurements on a femtosecond timescale probe the carrier and lattice dynamics of the material — a topic of high current interest because of the technological applications of high-speed electronics.

i. *Measurements on GaAs:* We have performed femtosecond melting experiments on GaAs using linear reflectivity and reflected second-harmonic radiation as probes of the melting process. These experiments exploit the strong nonlinearity of a non-centrosymmetric crystal to reveal dramatic changes in the electronic

response and in the atomic structure of the material within 200 fs of excitation. The measurements show that a phase change occurs before the ions in the lattice are thermal. The results are presented in detail in the Significant Accomplishment section at the end of this report.

ii. *Femtosecond nonlinear optical effects.* Coherent anti-Stokes Raman spectroscopy has been used to study the dynamics of vibrational energy transfer in transparent solids and liquids, where long interaction regions of the three input beams permit the growth of a sizeable anti-Stokes output beam in the forward direction. With highly absorbing semiconductors, however, transmission CARS is possible only on very thin samples. In analogy with the reflected second-harmonic signal of the GaAs experiments above, it is possible to produce a coherent output beam in reflection from strongly absorbing materials in which absorption provides resonant enhancement of the nonlinear signal. We are the first group to our knowledge to have seen a reflection CARS signal from an opaque material. Our preliminary studies of ZnSe and GaAs have indicated the extreme importance of intense, highly focusable input pulses of short duration. This observation opens the door to a whole new series of measurements involving nonlinear optical effects. In particular, we plan to directly monitor the phonon population during photoexcitation of semiconductor materials in order to learn more about electron-phonon interactions.

To facilitate these femtosecond nonlinear optical studies, we have undertaken a major upgrade of our femtosecond pulse amplifier. The goal was to increase the pulse energy available for melting and nonlinear optics experiments, and especially to improve the spatial profile of the beam. In addition to adding a fifth stage of amplification, we have replaced the final longitudinal amplifier cell with a large Bethune prism dye cell, making the entire amplifier chain transversely pumped. This corrects a problem with the original design in which the imperfect spatial profile of the pumping YAG laser was impressed on the amplified beam. The result

is an output beam with more than double the previous energy (2 mJ) and a smooth profile that focuses to a much tighter spot.

Because of the higher energy now available it will be possible to extend other laser melting experiments done previously under JSEP sponsorship to the femtosecond domain. An interesting candidate for study is the recently reported "molten" phase of graphite after irradiation with ultrashort laser pulses. While most semiconductors undergo a transition to a metallic state under laser melting, there has been disagreement as to whether the molten phase of graphite is metallic. An ellipsometric measurement at a single wavelength performed by us a few years ago, indicated a nonmetallic liquid phase [1]. For an unambiguous determination of the electrical properties of molten graphite, it is necessary to perform the ellipsometry over a broad range of wavelengths. This will determine the contributions of free and bound electrons to the dielectric function.

Reference:

1. A. M. Malvezzi, N. Bloembergen, C. Y. Huang, *Phys. Rev. Lett.*57, 146 (1986).

II.2 Laser Light Scattering from Surfaces and Monolayers. E. Mazur, D. S. Chung, and K. Y. Lee, Contract N00014-89-J-1023 and NSF DMR-8858075; Research Unit 7.

There has been a growing interest in recent years in the properties of Langmuir-Blodgett films, monolayers and surfactants because of the many technological applications of such systems, and because such mono-molecular layers can serve as models for the study of two-dimensional systems. In spite of this interest, viscoelastic properties of monolayers remain poorly understood. This is partly due to the lack of experimental results accurate enough to put the existing theories to a vigorous test. It has been known for a long time that wave attenuation on a free

water surface is enhanced by the presence of surface-active materials, because the viscoelastic properties of monolayers alter the dynamic properties of the interface. The aim of this project is to extract viscoelastic information of surface films from accurate damping measurements.

A major obstacle for getting accurate damping results has been that they cannot be obtained directly from laser light scattering measurements but require a complicated deconvolution processes with usually unknown instrumental functions. Using a novel Fourier transform heterodyning spectroscopy (FTHS) technique developed in our laboratory [1], we have developed an apparatus that can perform direct measurements of the spatial damping coefficients, without requiring a deconvolution or calibration. The apparatus probes the surface in two spots and employs a "phase-matched geometry" for the main laser beam and the local oscillator. With the new apparatus we achieve a world-record spectral resolution of 20 μHz [2].

To test our apparatus we first studied capillary wave damping at a clean air-water interface. An ultrapure water sample was sealed inside a chamber filled with pure nitrogen. Working in a clean environment is crucial for this experiment as any contamination of the interface greatly affects our results. Capillary waves of known frequencies are generated using electrocapillarity, and the wave amplitudes are monitored as a function of distance. We studied capillary waves in the frequency range 500–2000 Hz; for each frequency we obtained an exponential falloff of the amplitude with distance, in excellent agreement with the theoretical predictions.

Following this initial experiment, we measured the effect of a monolayer of pentadecanoic acid (PDA) on capillary wave damping at the air-water interface. Over the entire range of frequencies studied (500–2000 Hz), we observe a decrease in the wavevector as the surface concentration is increased. At low surface concentration, the measured damping coefficient obtained remains the same as the one for pure water, but as the concentration is increased to the liquid-expanded/gas (LE/G)

coexistence region, the damping coefficient increases dramatically. A maximum in damping is reached right at the transition point from the LE/G coexistence to the LE phase, after which it decreases again and finally levels off near the collapse of the film [3]. The exact reason for the location of such a maximum is still unknown and theoretical analysis of the new data is underway.

References:

1. D. S. Chung, K. Y. C. Lee, and E. Mazur, *Int. J. of Thermoph.*9, 729 (1988).

2. E. Mazur, D. S. Chung and K. Y. Lee in *Laser Spectroscopy IX*, eds. M. Feld, A. Mooradian and J. Thomas (Academic Press, Cambridge, 1989), 216.

3. K. Y. Lee, D. S. Chung and E. Mazur, *Phys. Rev. Lett.*, submitted.

ANNUAL REPORT OF

PUBLICATIONS/PATENTS/PRESENTATIONS/HONORS

d. Books (and sections thereof) Published

Second-harmonic efficiency and reflectivity of GaAs during femtosecond melting J.-K. Wang, P. Saeta , Y. Siegal, E. Mazur and N. Bloembergen, in Ultrafast Phenomena VII, Eds. C.B. Harris, E. Ippen and A.H. Zewail (Springer Verlag, 1990).

g. Invited Presentations at Topical or Scientific/Technical Society Conferences

N. Bloembergen, "Second Harmonic Conical Refraction," plenary lecture, Interdisciplinary Laser Science Conference (ILS-V), Stanford, August 1989.

N. Bloembergen, "Science and Technology Drive Each Other," MIT Dibner Institute Workshop on the Question of Technological Determinism, December 1989.

N. Bloembergen, "Historical Reminiscences about Nonlinear Optical Materials," US-USSR Binational Symposium, Irvine, CA January 1990.

N. Bloembergen, "Some Reminiscences about Nonlinear Optics," American Physical Society New England Section Meeting, Lowell, Massachusetts, April 1990.

N. Bloembergen, "Historical Reminiscences about Nonlinear Optical Materials," LEOS, April 1990.

N. Bloembergen, "Historical Reminiscences about Nonlinear Optical Materials," Nonlinear Optics '90 Conference, Kauai, HI, July 1990.

h. Contributed Presentations at Topical or Scientific/Technical Society Conferences

"Reflectivity and second harmonic efficiency of GaAs during femtosecond melting" J.-K. Wang, P. Saeta, Y. Siegal, E. Mazur, and Nicolaas Bloembergen, Ultrafast Phenomena Conference, Monterey, California, June 1990.

i. Honors/Awards/Prizes

N. Bloembergen served as President-elect of the American Physical Society in 1990 and will serve as President in 1991.

II.3 Multiphoton Vibrational Excitation of Molecules. E. Mazur, C.Z. Lü, K. H. Chen, S. Deliwala, and J. Goldman, Contract N00014-89-J-1023 and ARO DAAL03-88-K-0114; Research Unit 8.

In this research unit we continued the study of infrared multiphoton excited molecules in a free supersonic jet expansion using time-resolved broadband coherent Raman spectroscopy (CARS). Improvements were incorporated into many aspects of the experimental apparatus, including the CO_2-laser and streak camera timing synchronization, computer data acquisition and analysis, and the beam machine pulsed supersonic jet. One of the graduate students involved in this project, K. H. Chen, was the second student to obtain the Ph.D. degree on this project, with a thesis on spontaneous and coherent anti-Stokes Raman spectroscopy of infrared multiphoton excited molecules. Dr. Chen currently works at General Electric corporation.

The multiplex CARS apparatus was improved by 1) adding an extremely fast infrared detector and amplifier circuit with a response time of less than 10 ns, which allows accurate synchronization of the CO_2-laser pulse and the CARS probe to within 30 ns, making it possible to resolve short time dynamics of collisional energy exchange in the molecular jet, 2) optimization of the Hamamatsu streak camera performance and triggering, and implementation of a new method of data acquisition that allows one to obtain a set of spectra at different time delays all in a single camera image, which allows more accurate quantitative analysis of the data than previously possible, 3) modifying and characterizing the pulsed supersonic jet to obtain improved cooling and density characteristics, and 4) implementation of new software, coded by graduate student P. Saeta, which speeds data acquisition and provides new powerful image analysis techniques.

Interpretation methods for the CARS data also continue to move forward with the completion of a CARS spectrum simulation program. Based on the assumption

of thermal equilibrium within each normal mode of a molecule, the code generates accurate spectra which yield a much deeper quantitative insight into the dynamics of our experiments on vibrational and rotational CARS. Initial steps have also been completed into the development of a dynamical model of the molecular relaxation process, which will be combined with the existing code to create a complete simulation of our vibrational CARS experiments.

During this past year our efforts have concentrated on continuing the work started by Dr. Chen. Detailed measurements of infrared excited SF_6 at high and low collision rate conditions in the free jet expansion have yielded a new interpretation of spontaneous Raman and CARS work done with this molecule by previous researchers [1]. We found that spectral features previously attributed to collisionless laser excitation actually exhibit a very strong dependence on the molecular collision rate. Also, we discovered that earlier efforts at measuring the populations of each normal mode were inaccurate. Our present work yields results that are consistent with a conceptually simple model, and by using the code mentioned above, provides a more detailed quantitative picture of the dynamics of infrared excitation and relaxation. Theoretical analysis of is work is still underway and will be published shortly [2].

We are currently continuing work on the dynamics of the SF_6 system, and plan to apply our current model to some other molecular systems of differing size and spectral characteristics. We also plan to continue work on rotational Raman in a free jet, and on improving the performance characteristics of these jets. Other work will include investigation of electronic-vibration coupling in small molecules such as NO_2, eventually leading up to planned femtosecond investigations of molecular electronic and vibrational excitation dynamics.

References:

1. E. Mazur, C. Z. Lũ, S. Deliwala, and J. Goldman, IQEC '90 Proceedings.

2. C.Z. Lũ, S. Deliwala, J. Goldman, K. H. Chen, and E. Mazur, submitted to *Phys. Rev. Letters.*

II.4 Coherent anti-Stokes Raman Spectroscopy of Infrared Excited SO_2.

E. Mazur, C.Z. Lũ, S. Deliwala, and J. Goldman, Contract N00014-89-J-1023 and ARO DAAL03-88-K-0114; Research Unit 8.

A project related to the one described in Section II.3 is an investigation of the mechanism of multiphoton excitation of SO_2 [1]. The study of infrared multiphoton excitation of small polyatomic molecules such as SO_2 has received considerable attention in the literature. This molecule is representative of small size systems which, according to the quasicontinuum model, can be difficult to excite to high vibrational levels since the density of states at low excitation is relatively small. While observation of inverse electronic excitation in SO_2 clearly demonstrated that infrared multiphoton excitation to high vibrational levels is possible, these studies left unresolved the issue of which mode of the molecule is actually excited by the CO_2-laser. The ambiguity arises primarily because there is no available CO_2-laser line resonant with the ν_1-mode. The 9R(32) line is a strong CO_2-laser line close to ν_1-mode resonance; the 9P(32) line, on the other hand, is resonant with the first overtone of the ν_2-mode; and the 9R(22) line, one of the more intense CO_2 lines in the 9-μm region, lies between these two bands (71 cm^1 detuned from ν_1 and 44 cm^1 from $2\nu_2$). Because infrared multiphoton excitation is intensity dependent for a small molecule like SO_2, the strong 9R(22) line is historically the one most often utilized in the literature. It is not immediately clear, however, whether the ν_1 stretching mode or the $2\nu_2$ overtone band undergoes infrared multiphoton excitation when this line is used.

Using the time-resolved CARS setup described in the previous section we are able to directly observe the vibrational population in the various modes of the molecule. We determined that the ν_1-mode is excited, and that no detectable overtone pumping occurred under a large number of conditions, including tuning to the 9R(32), the 9P(32), and the 9R(22) CO_2-laser lines, a static gas cell and supersonic jet samples, and energy fluxes up to 3 J/cm^2.

It should be emphasized that our results show that both 9R(22) and 9R(32) pumping of SO_2 lead to excitation of the ν_1-mode at 1151.3 cm^1. While these lines are significantly detuned from the band head, they fall near the peak of the rotational Q-branch of the ν_1-mode at room temperature. This result should provide a clearer understanding of previous and future work in the field, and also illustrates the utility of the multiplex BOXCARS technique for direct observation of mode-selective excitation.

Reference:

1. C.Z. Lũ, J. Goldman, S. Deliwala, K. H. Chen, E. Mazur, submitted to *Chem. Phys. Letters.*

ANNUAL REPORT OF

PUBLICATIONS/PATENTS/PRESENTATIONS/HONORS

a. Papers Submitted to Refereed Journals (and not yet published)

C.-Z. Lü, J. Goldman, S. Deliwala, K.-H. Chen and E. Mazur, "Direct Evidence for ν_1-mode Excitation in the Infrared Multiphoton Excitation of SO_2, *Chem. Phys. Letters.*

K.-H. Chen, C.-Z. Lü, N. Bloembergen, and E. Mazur, "Multiplex Pure Rotational Coherent Anti-Stokes Raman Spectroscopy in a Molecular Beam," *J. Raman Spectroscopy.*

K.-H. Chen, C.-Z. Lü and E. Mazur, "Time-resolved Coherent Anti-Stokes Raman Spectroscopy of SF_6 in a Supersonic Jet, *J. Chem. Phys.*

b. Papers Published in Refereed Journals

K.-H. Chen, C.-Z. Lü, L. A. Avilés, E. Mazur, N. Bloembergen and M. J. Shultz, "Multiplex Coherent Anti-Stokes Raman Spectroscopy Study of Infrared-multiphoton Excited OCS," *J. Chem. Phys.*91, 1462 (1989). (Partial support by ARO DAAL03-88-K-0114)

c. Books (and sections thereof) Submitted for Publication

E. Mazur and C.-Z. Lü, "Nonlinear Spectroscopy of Infrared Multiphoton Excited Molecules," in *Resonances*, a volume in honor of the 70th birthday of Nicolaas Bloembergen, Eds. M. Levenson, E. Mazur, P. Pershan and Y.R. Shen (World Scientific, Singapore, 1990).

E. Mazur, C.-Z. Lü, S. Deliwala, and J. Goldman, "Coherent Anti-Stokes Raman Spectroscopy of Highly Vibrationally Excited Molecules in a Jet," Proc. XII Int. Conf. Raman. Spectr. (Wiley, New York, 1990).

d. Books (and sections thereof) Published

K.-H. Chen, C.-Z. Lü, E. Mazur, N. Bloembergen and M. J. Shultz, "Multiplex CARS Study of Infrared-multipphoton-excited OCS," in *Laser Spectroscopy IX*, eds. M. Feld, A. Mooradian and J. Thomas (Academic Press, Cambridge, 1989) 439.

E. Mazur, C.-Z. Lü, S. Deliwala, and J. Goldman, "Collisional and Intramolecular Dynamics of Low-Lying Vibrational States of Infrared Multiphoton Ex-

cited Molecules," *Tech. Digest*, XVII Int. Conf. on Quantum Electronics 8 (1990) 214. (Partial support by ARO DAAL03-88-K-0114)

g. **Invited Presentations at Topical or Scientific/Technical Society Conferences**

"Coherent Anti-Stokes Raman Spectroscopy of Highly Vibrationally Excited Molecules in a Jet," International Conference on Raman Spectroscopy, Columbia, S. Carolina, August 1990.

h. **Contributed Presentations at Topical or Scientific/Technical Society Conferences**

"Multiplex CARS Study of Infrared-multiphoton-excited OCS," Ninth International Conference on Laser Spectroscopy, Bretton Woods, New Hampshire, June, 1989.

"Collisional and Intramolecular Dynamics of Low Lying Vibrational States of Infrared Multiphoton Excited Moleculesi," Internationl Quantum Electronics Conference, Anaheim, California, June 1990. (Partial support from ARO DAAL03-88-K-0114)

i. **Honors/Awards/Prizes**

E. Mazur was elected Fellow of the American Physical Society

j. **Graduate Students and Postdoctorals Supported Under JSEP for the Year Ending July 31, 1990**

Dr. C.Z. Lü, and Messrs. J. Goldman, and K. H. Chen

III. INFORMATION ELECTRONICS: CIRCUITS AND SYSTEMS

Personnel

Assoc. Prof. J. J. Clark
Prof. Y. C. Ho
Dr. J. Q. Hu
Dr. L. Servi
Dr. S. Strickland
Dr. B. Zhang

Mr. K. Budka
Mr. L. Y. Dai
Mr. J. Feigen
Mr. D.J. Friedman
Mr. R. P. Hewes
Mr. L. Y. Shi

III.1 CMOS Current Mode Realizations of Neural Network Structures.

J. J. Clark, Contracts N00014-89-J-1023 and NSF-CDR-85-00108; Research Unit 9.

In this research program we are concerned with the development of analog CMOS circuits to be used in neural network systems. In particular we are interested in networks that can be used for the processing of sensory information. Towards this end we have been working on the following three projects:

1. CMOS Analog Self-Organizing Neural Networks

As described in the previous year's report we are investigating the design and construction of a self-organizing feedforward neural network which, in theory, exhibits behavior similar to the first few layers of the visual cortex in mammals. The basic structure of our current mode design combines analog current multiplier synapses and bidirectional current mirror summation elements with a weight updating circuit.

The weight update circuit computes a stochastic (if the input to the neuron is a random process) correlation between the input to the neuron and the output. If the correlation is high, the synaptic weight corresponding to the particular input

in question is increased. Conversely, if the correlation is low, the synaptic weight is decreased. We combine the correlation process, weight storage and weight updating in a single subsystem, a switched capacitor integrator. This circuit has two capacitors. The first integrates the input voltage over a period of time. The second acts as a hold or storage device. At the end of each integration period the charge on the integration capacitor is dumped onto the hold capacitor, thereby performing the update of the synaptic weight. As this switched capacitor integrator is such an important part of our analog neural elements, we fabricated test circuits in order to analyze their performance. These integrators were made in various sizes (different sized transistors), to see how small we could make them without losing functionality. The minimum useful size (of the integrator amplifiers, and not counting the area of the capacitors) was 40μ by 50μ. We also were able to examine the uniformity of the integrator (actually the operational amplifier) characteristics across the chip. It was found that the integrator to integrator variations in performance (hold time, offset voltages) were quite small and should not present problems in a neural network chip (especially in light of the fact that the self-organizing neural net is very insensitive to offsets and gain variations — they get learned as well). The hold times of the integrators were on the order of tenths of seconds. Thus the maximum integration time for the learning phase of the self-organizing neural net is about 10 milliseconds. This could cause a problem if the statistics of the input to the net are such that a long integration time is required for accurate determination of correlations. Longer integration times could possibly be obtained if one can handle the leakage of the integrator capacitor. Since the integrator is in a feedback loop, where the integrator output sets the gain applied to the signal going into the integrator, any droop in the final integrator output can be compensated by an increase in the gain (or synapse weight). This approach reduces the signal-to-noise ratio, and can only extend the integration time a moderate amount, since the droop in

the integrator voltage due to leakage is exponential. A potential problem with the switched capacitor integrator that was discovered after fabrication was the leakage of the switches in the integrator. This leakage (which was due to the reverse current of the source-substrate and drain-substrate junctions) caused both a slight increase in the droop rate and a poor isolation of the integration capacitor and the input voltage. Thus there will be some input-dependent charge transferred to the storage capacitor during the interval in which charge is being dumped from the integration capacitor to the storage capacitor. This could cause problems if we were using the integrator in a "sample-hold" configuration, but because we are dumping charge from the integration capacitor to the storage capacitor in a very short time compared to the integration time, the effect should be small. The leakage of the switches connected to the storage capacitor only contribute to the droop rate.

A CMOS chip containing a single 10 synapse neural element has been fabricated, although it has not yet been fully characterized and tested. The current mode neural element is a complex system and requires a significant amount of circuitry to test it. There are 5 bias voltages which have to be set for proper operation (and these voltages interact somewhat), there are 10 inputs to vary, and there are 2 clock signals whose relative timing is critical. We are currently in the process of constructing the test set. We have made some basic tests of the chip. The current mode input/output pads (which are essentially the same as a single input nonadaptive neural element) work as desired and, in particular, are very linear. As mentioned above, we verified the operation of the integrator circuits. The analog multiplier circuits used in the synapses were fabricated on a previous test chip and their operation verified. It was observed that, because of the current mode approach, the power dissipation of the neural elements is quite high. A single element dissipates 600 milliwatts. Thus, if we do not reduce the power consumption by some alteration of the circuit design, the planned 25 element chip would dissipate

15 watts. This is not feasible with the current packaging of the chips. Hence, we plan to redesign the circuit to reduce the power consumption. The majority of the current draw is by the summing junction of the neurons, the sum and difference blocks of the analog current multipliers and by the current mode input and output pads. We will therefore concentrate on bringing the current draw of these circuits to a more reasonable level.

2. Fixed Weight Analog Neural Network for Sensor Processing

Not all neural networks need to be adaptive to be useful. For example, the neural systems in the early levels of the mammalian visual system are more or less fixed in their functionality. The current mode approach used in the above adaptive feedforward network can be straightforwardly applied to implementing spatial filtering and feature extraction processes. To this end we have fabricated and tested spatial filtering (or convolution) circuits using the current mode neurons. These neurons were without the weight adaption circuitry, and used bidirectional current mirrors for current multiplication rather than the more complex analog current multipliers. We can do this since we do not need to change the synaptic weights. Our test spatial convolution chip showed that we can perform useful convolution operations (we implemented x and y derivative operators, as well as smoothing operators), as well as implement both positive and negative convolution coefficients (or in biological terms, excitatory and inhibitory synapses).

As these fixed-weight neural networks are intended for sensory information processing tasks we have investigated combining these on chip with sensors of various kinds. We have fabricated a test chip that contain both magnetic sensors and spatial filters. This chip did not work as desired due to problems with the offset voltage of the magnetic sensors. We have a new design which should solve this problem. We will send this chip out for fabrication in the near future. We have also fabricated a test chip containing phototransistors. These photo-sensitive devices

will be used in the active sensor chip described below. These devices were the same as described by Carver Mead. Our measurements on the fabricated devices showed that they had high sensitivity and the desired logarithmic response.

3. Hybrid Architecture for Active Sensor Chips

We are working on a novel application of our current-mode neural-network-based sensory information processing circuits. This is the active sensor chip. This device, unlike standard sensors which output a steady stream of sensory data (like the video signal of a solid state TV camera), outputs motor commands. Such a chip would find application in small autonomous robots, whose behavior (motor activity) depends on the data that it senses. We have developed a hybrid (both analog and digital) architecture for such sensing devices. The digital part of the device performs the "reasoning" which prioritizes the current goals of the system and determines the proper motor action to be taken based on the current sensory data. This digital "reasoning" system is a finite state machine which essentially chooses the output of one of a number of analog modules that convert sensor data into desired motions. For example, one module may be concerned with line finding, so it performs edge detection (using the current mode convolver), determines the edge direction and outputs this as the desired direction of motion. We have developed a software simulator of a general active sensor chip which allows us to develop the "program" (i.e., the state transition diagram of the finite state machine) that results in a given system "behavior" (how the system responds to a given sensory stimulus). We plan in the future to implement a simple instantation of such an active sensing device in CMOS, using the current mode analog neural networks that we have developed as well as more standard digital implementations of finite state machines.

ANNUAL REPORT OF

PUBLICATIONS/PATENTS/PRESENTATIONS/HONORS

a. Papers Submitted to Refereed Journals (and not yet published)

J.J. Clark, "Split Drain MOSFET Magnetic Sensor Arrays," *Sensors and Actuators*, (to be published in Vol. A-24, No. 2, pp. 107–116) (Partially supported by NSF CDR–85–00108)

g. Invited Presentations at Topical or Scientific/Technical Society Conferences

J.J. Clark, University of Maryland, Systems Research Center Research Review Symposium, May 1990.

J.J. Clark, MIT Artificial Intelligence Laboratory, March 1990.

J.J. Clark, SPIE Visual Communication and Image Processing IV, Philadelphia, November 1989.

h. Contributed Presentations at Topical or Scientific/Technical Society Conferences

J.J. Clark and D.J. Friedman, "Local Processing of Sensor Array Data Using Current Mode Circuitry", Proceedings of the 1989 International Electron Devices Meeting, Washington D.C., December 1989, pp. 507–510.

J.J. Clark, "An Analog CMOS Implementation of a Self-organizing Feedforward Network," Proceedings of the 1990 International Joint Conference on Neural Networks, Washington D.C., January 1990, pp. II–118–121 (Partially supported by NSF CDR–85–00108).

j. Graduate Students and Postdoctorals Supported Under JSEP for the Year Ending July 31, 1990

Mr. D.J. Friedman (NSF Scholar, no salary support), and Mr. R.P. Hewes

III.2 Decision and Control — Discrete Event Dynamic Systems Study.
Y. C. Ho, Grant N00014-89-J-1023, Contracts ONR-N00014-86-K-0075, NSF-ESC-85-15449, NSF-CDR-88-03012, and DAAL-03-86-K-0171; Research Unit 10.

In 1989–90 we continued our research in Discrete Event Dynamic Systems (DEDS) and Perturbation Analysis (PA). On the theory side, a rather complete and satisfying picture of the unbiasedness and consistency of PA estimates is emerging in a series of papers by Glasserman, Hu, and Strickland (see publication lists below). At the same time, specific advances on the theory of second derivative PA estimates for various versions of single queue-server combinations have been carried out. Two books in a book series dedicated to the subject are now scheduled for publication in 1990. An international Journal on DEDS has been launched. All of these testify to the acceptance and growth of the subject matter which the Harvard group played a leading part in creating.

We also developed a new algorithm for the performance gradient estimation of very very large arbitrary Markov Chains (with state space of the order of one billion). This is a feat that has never been done before. As a corollary, these results make practical the application of likelihood ratio (LR) method to DEDS. Previously, variance problems have plagued the LR method. The technique developed is a generalization of the regenerative segmentation idea but allows the direct control of segment length, and hence variance growth.

On the application side, we are applying the PA methodology to the FDDI (Fiber Optic Distributed Data Interface) problem in telecommunication networks. FDDI will become a standard interface for computer-communication systems. Its performance analysis so far, however, has been largely approximate or via brute force simulation. We hope to use PA techniques to enhance the efficiency of simulation.

ANNUAL REPORT OF

PUBLICATIONS/PATENTS/PRESENTATIONS/HONORS

a. Papers Submitted to Refereed Journals (and not yet published)

M. C. Fu and J. Q. Hu, "On Smoothed Perturbation Analysis for Second Derivative Estimation of the GI/G/1 Queue," submitted to *IEEE Transaction on AC.*

M. C. Fu and J. Q. Hu, "Second Derivatives in Multi-Server Queueing Systems," submitted to *Management Science.*

J. Q. Hu and M. C. Fu, "Second Derivative Sample Path Estimators for the GI/G/m Queue," submitted to *Management Science.*

J. Q. Hu, "Sample Path Performance Analysis of Discrete Event Dynamic Systems," submitted to *IEEE Transaction on AC.*

J. Q. Hu, "Infinitesimal Perturbation Analysis for Queueing Systems with Load-Dependent Service and/or Arrival Rates," submitted to *Queueing Systems.*

L. D. Servi, "A Network Flow Approach to a Satellite Scheduling Program," submitted to *Operations Research.*

L. D. Servi and J. Keilson, "Networks of Non-homogeneous M/G/∞ Systems," submitted to *Performance Evaluation.*

B. Zhang, "Stochastic Approximation Method for Solving Linear Equations Arising in Markov Chain Models," submitted to *ORSA J. on Computing.*

B. Zhang, "A Stochastic Recursive Algorithm for Gradient Estimation," submitted to *Applied Probability.*

B. Zhang and Y. C. Ho, "Performance Gradient Estimation for Very Large Markov Chains," submitted to *IEEE Trans. Automatic Control*

B. Zhang and Y. C. Ho, "Likelihood Ratio Methods Using A-segments," submitted to *Performance Evaluation.*

J. Q. Hu and M. C. Fu, "Consistency of Infinitesimal Perturbation Analysis for the GI/G/m Queue," accepted in *European Journal of Operational Research*, 1990.

J. Q. Hu, "Convexity of Sample Path Performances and Strong Consistency of Infinitesimal Perturbation Analysis Estimates," accepted in *IEEE Transaction*

on AC, 1990.

J. Q. Hu, "Strong Consistency of Infinitesimal Perturbation Analysis for the GI/G/G1 Queue," accepted in *Management Science*, 1990.

J. Q. Hu, "On Steady-State Sample Path Derivative Estimates," accepted in *Applied Mathematics Letters*, 1990.

J. Q. Hu and S. Strickland, "Strong Consistency of Sample Path Derivative Estimates," accepted in *Applied Mathematics Letters*, 1990.

J. Q. Hu and M. C. Fu, "Bias Properties of Infinitesimal Perturbation Analysis for Multi-Server Queues," accepted in *Proceedings of Winter Simulation Conference*, 1990.

J. Q. Hu and Y. Wardi, "Strong Consistency of Infinitesimal Perturbation Analysis for Tandem Queueing Networks," accepted in *Journal of Discrete Event Dynamic Systems*, 1990.

b. Papers Published in Refereed Journals

M. C. Fu and J. Q. Hu, "Variance Properties of Second Derivative Perturbation Analysis Estimators for Single-Server Queues," *Proceedings of American Control Conference*," 1040–1041 (1990).

M. C. Fu, "On the Consistence of Second Derivative Perturbation Analysis Estimators for the M/G/1 Queue, *Applied Mathematics Letters*, 2(2), 193–197 (1989).

Y. C. Ho, "Recent Developments in Perturbation Analysis" Proceedings of the IFAC Workshop on Decision Making in Manufacturing Automation, Pergamon Press, Sept. 1989.

Y. C. Ho and J. Q. Hu, "An Infinitesimal Perturbation Analysis Algorithm for a Multiclass G/G/1 Queue," *Operations Research Letters*, 9, 35–44 (1990).

Y. Wardi and J. Q. Hu, "Strong consistency of Infinitesimal Perturbation Analysis for Networks with Correlated Service Times," *Proceedings of American Control Conference*, 1028–1033 (1990).

S. Strickland and C. G. Cassandras, "Observable Augmented Systems for Sensitivity Analysis of Markov and Semi-Markov Processes," *IEEE Trans. on Automatic Control*," 34(10), 1026–1037 (1989).

Y. C. Ho and X. Cao, "Models of Discrete Event Dynamic Systems," *IEEE Control Systems Magazine*, 10(4), 69–76 (1990).

c. **Books (and sections thereof) Submitted for Publication**

Y. C. Ho and X. Cao, *Perturbation Analysis of Discrete Event Dynamic Systems* (Kluwer Publishing Company, 1990).

g. **Invited Presentations at Topical or Scientific/Technical Society Conferences**

Y. C. Ho, First PA Workshop, Wolfeboro, N. H., August 4–6, 1989.

Y. C. Ho, Genoa-IFAC Talk, September 18, 1989.

Y. C. Ho, SIAM Detroit Chapter Annual Conference, October 21, 1989.

Y. C. Ho, University of Texas, Mfg. System Eng. Program, November 6, 1989.

Y. C. Ho, Mitre Corporation, Washington, D.C., November 16, 1989.

Y. C. Ho, Texas System Theory Conference, Rice University, November 18, 1989.

Y. C. Ho, University of Texas, ECE Department, November 20, 1989.

Y. C. Ho, CDC Survey Talk, December 10, 1989.

Y. C. Ho, CDC Contributed Paper Talks, December 11, 1989.

Y. C. Ho, 28th IEEE Conf. on Decision and Control, Tampa, FL., December, 1989.

Y. C. Ho, MIT Army Review, March 16, 1990.

Y. C. Ho, "Models for Innovation" Conference Plenary Address, Rome, Italy, March 23, 1990.

Y. C. Ho, Harvard Alumni, April 21, 1990.

Y. C. Ho, University of Maryland, SRC Research Review, May 4, 1990.

Y. C. Ho, Aberdeen Proving Ground, AMSAA, June 5, 1990.

Y. C. Ho, US/Japan Mfg. Research Exchange, Nagoya, Japan, July 26, 1990.

Jian-Qiang Hu, DEDS Workshop at University of California at Berkeley, May 20, 1989.

Jian-Qiang Hu, The University of Massachusetts at Amherst, November 7,

1989.

L. D. Servi, Texas A&M University, Industrial Engineering Department's Distinguished Lecture Series, October, 1989.

L. D. Servi, Joint National ORSA/TIMS Conference, New York, October, 1989.

i. Honors/Awards/Prizes

Y. C. Ho was appointed Editor-in-chief of the new *International Journal on Discrete Event Dynamic Systems.*

Y. C. Ho was invited to be Associate Editor of the new journal on *Mathematical Systems and Control.*

j. Graduate Students and Postdoctorals Supported Under the JSEP for the Year Ending July 31, 1990.

Drs. Les Servi, S. Strickland, Bin Zhang, J. Q. Hu and Messrs. K. Budka, L. Y. Shi, J. Feigen, and L. Y. Dai.

IV. ELECTROMAGNETIC PHENOMENA

Personnel

Prof. T. T. Wu
Prof. R. W. P. King
Dr. J. M. Myers
Dr. H.-M. Shen
Mr. G. Fikioris
Mr. D. K. Freeman
Ms. M. Owens
Ms. B. H. Sandler

Research in the area of electromagnetic radiation is directed toward the solution of practical problems through the complete understanding of the underlying physical phenomena. This involves the coordinated application of modern analytical, numerical, and experimental techniques and the use of high-speed computers and precision instrumentation. Application is also made of modeling techniques and the principle of similitude. Most practically significant problems in the area are sufficiently complicated that extensive computation and measurement are often required to justify approximations that are usually necessary. Where possible, general formulas are obtained and verified experimentally so that the phenomenon under study can be understood physically in analytical form and not just as a set of numbers.

The researches are concerned primarily with the properties of antennas and arrays and of the electromagnetic fields they generate in various practically important environments that lead to difficult problems with complicated boundary conditions. Examples include dipoles, insulated antennas, traveling-wave antennas and arrays, crossed dipoles, and loops near the boundary between two media such as air and the earth or sea, or the oceanic crust and sea water; the properties of lateral electromagnetic waves; remote sensing with lateral waves from the surface of the earth or sea, the arctic ice or the sea floor; lateral waves and reflected

waves in horizontally-layered media; the generation, propagation, and reception of lateral electromagnetic pulses; arrays of antennas along curved lines; and solitary electromagnetic pulses with slow rates of decay.

IV.1 Analytical and Numerical Determination of the Fields of Antennas near an Interface Between Two Half-Spaces with Significantly Different Wave Numbers.

T. T. Wu, R. W. P. King, B. H. Sandler, and M. Owens, Grant N00014-89-J-1023; Research Unit 11.

In 1982, King [1] derived simple formulas for the electromagnetic field of a vertical electric dipole that are valid everywhere in the earth (Region 1) and on the boundary with air (Region 2), when the dipole is also on the boundary in either region or at depth d in the earth. The following conditions were imposed:

$$|k_1^2| \gg |k_2^2| \quad \text{or} \quad |k_1| \geq 3|k_2|, \tag{1a}$$

and, on the surface-wave terms,

$$\rho^2 \gg |z|^2; \quad \rho^2 \gg d^2, \tag{1b}$$

where $k_1 = \beta_1 + i\alpha_1 = \omega[\mu_0(\epsilon_1 + i\sigma_1/\omega)]^{1/2}$ and $k_2 = \omega(\mu_0\epsilon_0)^{1/2} = \omega/c$ are the wave numbers of the two half-spaces.

Recently the electromagnetic field generated by the vertical electric dipole has been determined when the dipole is at any height in the air [2]. Simple explicit new formulas are derived in closed form for the three components of the electromagnetic field in the air. They show that the surface waves constitute the entire far field along the air-earth boundary ($\Theta = \pi/2$). Far from the boundary the surface wave is negligible and the field is accurately given by the direct and image terms. An important generalization in the derivation of the new simple formulas for the components of the electromagnetic field is the extension of their range of validity to *any point* in the air when the dipole is at a height d also in the air. Exact formulas are

obtained for the direct and image fields; the surface-wave terms are derived subject only to the condition (1a). The restrictions (1b) are eliminated so that the new formulas give the field everywhere, i.e., at all values of ρ and z, except at points very close to the dipole.

References:

1. R. W. P. King, "New Formulas for the Electromagnetic Field of a Vertical Electric Dipole in a Dielectric or Conducting Half-Space near its Horizontal Interface," *J. Appl. Phys.* 53, 8476–8482 (1982); Erratum, 56, 3366 (1984).

2. R. W. P. King, "Electromagnetic Field of a Vertical Dipole Over an Imperfectly Conducting Half-Space," *Radio Science* 25, 149–160 (1990).

IV.2 On the Radiation Efficiency of a Vertical Electric Dipole in Air Above a Dielectric Half-Space. R. W. P. King, B. H. Sandler, and M. Owens, Grant N00014-89-J-1023 and MITRE Corp. Project No. 91260; Research Unit 11.

A study of the fraction of power that remains in the air (upper half-space) and the fraction that is transferred into the earth (lower half-space) when the radiating source is a vertical dipole at a height d in the air has been completed [1]. The power P radiated by the dipole was separated into two parts by Hansen [2]: a part P_a that remains in the air, and a part P_g that is transferred into the earth. Hansen introduced this division of power in order to define the *radiation efficiency* as $\eta = P_a/(P_a + P_g)$. This is the fraction of the power radiated by the dipole that remains in the upper half-space. Since it appears superficially obvious that radio transmission between antennas in the air depends on the power that remains in the upper half-space, it seems reasonable to assume that the most desirable antenna is one that has the highest radiation efficiency. Actually, this ignores the important fact that power ultimately transferred to the earth at large radial distances is available in the air at all shorter distances.

The determination of the power in each region as a function of the height d of

the dipole involves not only direct, reflected, and refracted or transmitted waves, but also a surface wave that travels along the boundary in the air. The newly derived formulas [3] for the electromagnetic field in air of a vertical electric dipole at the height d in air—described under the previous topic—show that, when $d \sim 0$, the entire field along the surface of the earth is given by a surface wave that propagates along the boundary in the air and transfers power into the earth as it travels. The surface wave is shown to contribute a major part of the low-angle field needed for over-the-horizon radar. Since all the power associated with the surface wave is transferred into the earth, an antenna that generates a large surface wave—like the vertical dipole on the earth—must have a low radiation efficiency.

Hansen's numerical evaluation [2] of the radiation efficiency of the vertical electric dipole indicated that P_g grows without limit as the height d of the dipole is reduced to zero. This means that P_a and the radiation efficiency both vanish as $d \rightarrow 0$. In [1], the radiation efficiency as defined by Hansen has been reformulated and evaluated analytically for a dielectric earth. It is shown that the radiation efficiency decreases to a small value when $d \rightarrow 0$, but not to zero as obtained numerically by Hansen.

An antenna with high radiation efficiency in the sense defined by Hansen [2] necessarily must generate a very weak surface wave. On the other hand, an antenna that generates a strong low-angle field with a significant value along the boundary surface, $\Theta = 90°$, necessarily generates a strong surface wave that transfers all the power associated with it into the earth. The design of an antenna that maximizes the surface wave and the entire low-angle field in the range $80° \leq \Theta \leq 90°$ is a problem of considerable interest. Such an antenna will have a low radiation efficiency and most of the power radiated will not remain in the upper half-space (air) but will be transferred to the lower half-space (earth). It may be concluded that the concept of radiation efficiency as defined by Hansen is not a useful figure-of-merit.

References:

1. R. W. P. King, "On the Radiation Efficiency and the Electromagnetic Field of a Vertical Electric Dipole in the Air Above a Dielectric or Conducting Half-Space," *J. Electromagn. Waves & Appl.*, accepted for publication.

2. P. Hansen, "The Radiation Efficiency of a Dipole Antenna Located Above an Imperfectly Conducting Ground," *IEEE Trans. Antennas Propagat.* AP-20, 766–769 (1972).

3. R. W. P. King, "Electromagnetic Field of a Vertical Dipole Over an Imperfectly Conducting Half-Space," *Radio Science* 25, 149–160 (1990).

IV.3 The Propagation of Signals Along a Three-Layered Region: Open Microstrip.

R. W. P. King, B. H. Sandler, M. Owens, and T. T. Wu, Grant N00014-89-J-1023; Research Unit 11.

A rigorous approach to the analysis of microstrip circuits involves complicated integrals that must be solved numerically. An alternative is to seek a fundamental understanding of the nature of electromagnetic-wave propagation in microstrip by obtaining simple analytical approximations of the integrals in a manner similar to that carried out for the problem of two electrically different half-spaces. Actually microstrip is a special three-layered region and some of its properties can be investigated in terms of the electromagnetic field generated by a unit horizontal electric dipole on the air-dielectric surface. Of primary interest in microstrip circuits and antennas is the electric field at the air-dielectric boundary and in the air above it, when the horizontal dipole is on the boundary.

During this reporting period, a new analysis has been completed in which the unit horizontal dipole is assumed to be in the air on the surface of the dielectric. Formulas for the field have been calculated from the exact integrals subject to the inequalities $k_0^2 < |k_1^2| \ll |k_2^2|$, where k_0 is the wave number of air, k_1 the wave number of the dielectric substrate, and k_2 the wave number of the conducting base. The complicated integrals for the electromagnetic field are greatly simplified if an approximation is made at the outset that does not alter the fundamental

properties. The approximation is to assume that the highly conducting base—Region 2—is perfectly conducting. Complete expressions for the six cylindrical components of the electromagnetic field in air of a horizontal electric dipole at the height d' over a dielectric-coated conducting plane have been obtained. Their application to determine the complete field of a microstrip patch antenna is in progress.

A comparison shows that the surface wave in the air above the substrate in microstrip is closely related to the surface wave in the air above a dielectric half-space. The amplitude is modified by the factor $(-ik_1 l)$ or multiples thereof, where l is the thickness of the dielectric substrate. The presence of the conducting half-space at the small distance l from the air-dielectric boundary eliminates propagation with the wave number k_1 in the dielectric, and provides the amplitude factors in powers of $(-ik_1 l)$. In effect, the surface wave that propagates in the air along the air-dielectric boundary is unaffected except in amplitude by the presence of the conducting half-space at all radial distances from the source smaller than $\rho \sim k_1^2/k_0^2$.

Studies of the fields generated by the pulse excitation of a horizontal dipole on the air-substrate boundary of microstrip are also being investigated [1]. Recent work has shown that the presence of the dielectric substrate significantly affects the vertical component of the electric-field pulse. In the absence of the dielectric layer, the decrease in amplitude with radial distance is extremely rapid for $E_z \sim 1/\rho^2$ and even more so for $E_\rho \sim 1/\rho^3$. With the dielectric present, both E_z and E_ρ decrease slowly with increasing distance— $\sim 1/\rho$. The shape of the E_z pulse in the absence of the dielectric layer is essentially the superposition of a positive Gaussian pulse and a reflected negative, slightly delayed Gaussian pulse. In the presence of the dielectric layer, the shape of E_z is obtained from the superposition of a pulse with the shape of the derivative of a Gaussian pulse and a similar reflected negative and slightly delayed pulse. This is readily understood if it is recalled that the leading $1/\rho$ term

in the surface-wave pulse generated on the boundary between two dielectric half-spaces by a Gaussian current pulse in a horizontal electric dipole is the derivative of a Gaussian pulse [2]. The $1/\rho$ field of the surface wave propagates as the derivative of a Gaussian pulse; the $1/\rho^2$ field of the direct field in air propagates as a Gaussian pulse. In the presence of a conducting half-space, both are reflected and the delayed reflected pulse combines with the direct fields to produce the final pulse shapes.

References:

1. R. W. P. King, "Lateral Electromagnetic Waves and Pulses on Open Microstrip," *IEEE Trans. Microwave Theory & Tech.* 38, 38–47 (1990).

2. R. W. P. King, "Lateral Electromagnetic Pulses Generated on a Plane Boundary Between Dielectrics by Vertical and Horizontal Dipole Sources with Gaussian Pulse Excitation," *J. Electromagn. Waves & Appl.* 3, 589–597 (1989).

IV.4 Lateral Electromagnetic Waves from a Horizontal Antenna for Remote Sensing in the Ocean. R. W. P. King, *Grant N00014-89-J-1023*; Research Unit 11.

The method developed earlier [1], [2] for finding a buried metal cylinder in the earth can be adapted to the search for cylindrical metal objects like mines and submarines in the ocean or lying on the sea floor. Because salt water has quite different properties from earth, both the theoretical adaptation and the practical application of the method involve significant modifications that are scientifically interesting. These include the following: (a) The fluid nature of water makes it possible to locate and move both the transmitting and receiving antennas, not in the air, but in the same medium as the cylinder to be located. This greatly increases the magnitude of the receivable scattered signal and significantly reduces the possible interference by reflections from the ionosphere, because the transmission coefficient of a plane wave normally incident on the surface of the sea from the air is very small at the frequencies involved. (b) The much higher conductivity of the

sea water compared to earth leads to a much greater complex wave number for electromagnetic waves. The associated wavelength is much shorter than that in the earth at the same frequency. It follows that a much lower frequency must be used in order to have the scattering cylinder with length $2h$ near resonance. Associated with the use of a lower frequency is a helpful decrease in the exponential attenuation of a traveling wave and a disadvantageous shift in the properties of lateral waves from those of the intermediate field with a radial decrease with distance of ρ^{-1} to the near field with a radial decrease of ρ^{-3}. Account is readily taken in the analysis of these important facts. A systematic study has been made [3] of the several important factors involved in the development of a method for locating submerged submarines from measurements of the scattered electromagnetic field at the surface. These involve the properties of crossed antennas in the sea at very low frequencies and the circularly polarized lateral-wave fields they generate, as well as the field scattered by a submarine and a crossed receiving antenna to detect this. Representative calculations are made to illustrate the relative orders of magnitude of the dimensions and fields involved and the required sensitivity of a receiver.

References:

1. R. W. P. King, "Scattering of Lateral Waves by Buried or Submerged Objects. I. The Incident Lateral-Wave Field," *J. Appl. Phys.* 57, 1453–1459 (1985).

2. R. W. P. King, "Scattering of Lateral Waves by Buried or Submerged Objects. II. The Electric Field on the Surface Above a Buried Insulated Wire," *J. Appl. Phys.* 57, 1460–1472 (1985).

3. R. W. P. King, "Lateral Electromagnetic Waves from a Horizontal Antenna for Remote Sensing in the Ocean," *IEEE Trans. Antennas Propagat.* 37, 1250–1255 (1989).

IV.5 Lateral Electromagnetic Pulses Generated by Horizontal and Vertical Dipoles on the Boundary Between Two Dielectrics. T. T. Wu and R. W. P. King, Grant N00014-89-J-1023; Research Unit 11.

In a recent paper [1] formulas are derived for the transient field generated by a vertical electric dipole on the boundary between air [Region 2; $k_2 = \omega(\mu_0\epsilon_0)^{1/2}$] and a dielectric half-space [Region 1; $k_1 = \omega(\mu_0\epsilon\epsilon_0)^{1/2}$] when excited by a Gaussian pulse. The time-domain formulas are obtained by Fourier transformation of the corresponding steady-state formulas. Since these are approximate in the sense that the permittivity of the dielectric is assumed to be large compared with that of air, the transient formulas derived from them do not include a second, much smaller pulse that travels in the dielectric and arrives much later than the main lateral pulse that travels in the air. This leaves some uncertainty about the accuracy of the approximate transient formulas at and near the time of arrival of the second pulse.

A new paper [2] has been written to obtain the exact field so that this question can be clarified. Since an exact formula is available for the vertical component of the electric field when the vertical dipole is excited by a delta-function pulse [3], this can be applied to obtain the corresponding component of the transient field with Gaussian-pulse excitation. The resulting integral has been evaluated numerically and compared with the approximate field. The agreement is very good. The only differences are a somewhat more rounded minimum and somewhat sharper maximum in the exact pulse and the nonappearance of the relatively small second pulse in the approximate field.

The question about the second pulse that travels in the dielectric and arrives at a later time is completely resolved in the exact solution. The second pulse is seen to arrive at the predicted time, and to have a Gaussian shape with an amplitude that is very much smaller than that of the first pulse, as expected. An important insight

gained from the approximate formulas is an explanation of the quite different shapes of the two pulses. The first pulse is dominated by the derivative of the Gaussian pulse with its $1/\rho$ amplitude factor. The Gaussian term has the amplitude factor $1/\rho^2$, so that it decays much more rapidly with increasing radial distance. Since the second pulse has the Gaussian shape, it must also be a $1/\rho^2$ term—but it is missing from the approximate formulas.

Since the transient field calculated by Fourier transformation of the approximate steady-state formulas gives accurate results for the vertical dipole except for the nonappearance of the small second pulse, the same should be true of the very similar field of the horizontal dipole on the boundary $z = 0$ in the dielectric. The corresponding approximate formulas are derived in [2] for the electric field of a horizontal dipole. It is seen that the transient field on the boundary surface generated by a single Gaussian current pulse consists of two outward traveling pulses. One travels in the air with the velocity c, the second travels in the dielectric with the velocity $c\epsilon^{-1/2}$. Except close to the source, the dominant part of the pulse in air consists of the $1/\rho$ terms in $E_{2z}(\rho, \phi, 0; t)$ and $E_{2\rho}(\rho, \phi, 0; t)$. These have the form $2\tau' \exp(-\tau'^2)$ of the derivative of the Gaussian pulse $\exp(-\tau'^2)$. The dominant part of the pulse in the dielectric consists of the $1/\rho^2$ terms in all three components. The $1/\rho^3$ terms constitute the static field due to the charges left on the ends of the dipole. This field remains after both pulses have traveled to infinite distance.

References:

1. R. W. P. King, "Lateral Electromagnetic Pulses Generated by a Vertical Dipole on a Plane Boundary Between Dielectrics," *J. Electromagn. Waves & Appl.* 2, 225–243 (1988).

2. R. W. P. King, "Lateral Electromagnetic Pulses Generated on a Plane Boundary Between Dielectrics by Vertical and Horizontal Dipole Sources with Gaussian Pulse Excitation," *J. Electromagn. Waves & Appl.* 3, 589–597 (1989).

3. T. T. Wu and R. W. P. King, "Lateral Electromagnetic Pulses Generated by

a Vertical Dipole on the Boundary Between Two Dielectrics," *J. Appl. Phys.* 62, 4345–4355 (1987).

IV.6 Lateral Electromagnetic Waves (Manuscript for Book). R. W. P. King, T. T. Wu, M. Owens, and B. H. Sandler, Grant N00014-89-J-1023; Research Unit 11.

It has become a tradition in the publication of researches in the area of electromagnetic phenomena to periodically summarize and coordinate major segments in book form. Accordingly, a manuscript is in preparation which contains the results of current and past researches on lateral electromagnetic waves that have been supported in large part by the Joint Services Electronics Program. The book is entitled "Lateral Electromagnetic Waves: Theory and Applications to Communication, Geophysical Exploration, and Remote Sensing." It has been accepted for publication by Springer/Verlag and is very near completion. The chapter headings are: 1. Historical and Technical Overview of Electromagnetic Surface Waves; Introduction to Lateral Waves, 2. Electromagnetic Preliminaries, 3. The Electromagnetic Field of a Unit Vertical Electric Dipole in the Presence of a Plane Boundary, 4. Applications of the Theory of the Vertical Dipole Near The Boundary Between Two Half-Spaces, 5. The Electromagnetic Field of a Horizontal Electric Dipole in the Presence of a Plane Boundary, 6. Interference Patterns; Comparison of Approximate Formulas with General Integrals and Measurements, 7. Applications of the Theory of the Horizontal Dipole Near the Boundary Between Air and Earth or Sea, 8. The Measurement of the Conductivity of the Oceanic Lithosphere with a Horizontal Antenna as the Source, 9. Lateral Waves in a One-Dimensionally Anisotropic Half-Space, 10. The Propagation of Lateral Electromagnetic Waves in Air over Vertical Discontinuities, 11. The Horizontally Layered Half-Space, 12. The Three-Layer Problem for Sediment on the Oceanic Crust, 13. Lateral Electromagnetic Pulses Generated by Vertical Dipoles, 14. Approximate Formulas for Lateral Electromagnetic Pulses

Generated by Vertical and Horizontal Electric Dipoles, 15. The Propagation of Signals Along a Three-Layered Region: Open Microstrip, 16. Antennas in Material Media Near Boundaries: The Bare Metal Dipole, 17. Antennas in Material Media Near Boundaries: The Terminated Insulated Antenna, 18. The Wave Antenna.

IV.7 Theoretical Study of Electromagnetic Pulses with a Slow Rate of Decay. T. T. Wu, J. M. Myers, H. M. Shen, and R. W. P. King, Grant N00014-89-J-1023, Army LABCOM Contract DAAL02-89-K-0097, and DOE Grant DE-FG02-84ER40158; Research Unit 11.

The interesting possibility of generating electromagnetic pulses of finite total radiated energy that can deliver energy to a distant receiver that decreases with distance much more slowly than the usual r^{-2} is being investigated both theoretically (this topic) and experimentally (see Topic IV.8). Such pulses are conveniently referred to as electromagnetic (EM) missiles [1]. Such electromagnetic missiles can be generated by any of a class of current distributions over one or another set of points contained in a bounded region of a two-dimensional or three-dimensional space. For a given current-bearing set of points as a transmitter, one can explore various time and space dependencies of the transmitting current. Over some classes of dependencies, the energy reaching the receiver decreases as $r^{-\epsilon}$, where ϵ is a positive number that can vary from one current to another. Current-bearing sets so far explored have dimension 0, 1 or 2. For these, the requirement of finite total radiated energy establishes a greatest lower bound on ϵ, dependent on the dimensions of both the set and the space in which it resides. This infimum defines what can be called the *pulse index* of a set relative to the space containing it. One might conjecture that the pulse index can be defined for sets of fractional Hausdorff dimension. In a new paper [2] it is shown that this is so, and that for certain sets of fractional dimension, the index is related to the dimension just as it is for integral dimensions.

The theoretical analysis of various electromagnetic-missile launchers has con-

tinued during this period with the investigation of the spherical reflector illuminated by a point source [3]. This structure too is found to be capable of launching an electromagnetic missile. Since the surfaces of the reflector are not complete spherical surfaces, the problem cannot be solved by simple boundary matching. The electromagnetic fields have to be solved in three regions separately. The general solutions are matched on the boundaries to obtain a set of coefficient equations. Under the conditions for an electromagnetic missile, the coefficient equations are solved asymptotically. The evaluation of the Poynting vector shows that the energy radiated from the reflector has the same slow rate of decay as for the spherical lens. An analysis of the spherical reflector as a possible launcher of curved electromagnetic missiles [4] is under consideration.

Also during this period, the echo backscattered when an EM missile encounters a plate target has been studied [5]. Conventional radar pulses spread so that the energy reaching a reflecting target at range r decreases as r^{-2}. The energy echoed from the target also decreases as r^{-2}, so that the energy backscattered to the transmitter is proportional to the product, i.e., to r^{-4}. Pulses of finite total energy that satisfy Maxwell's equations need not decrease as r^{-2}, but can instead decrease much more slowly, for instance as $r^{-\epsilon}$ where ϵ is a positive number that can be chosen as small as one pleases. By analogy with conventional radar, one expects the energy of the backscattered echo of an EM missile to be proportional to $r^{-2\epsilon}$. Instead, the reflector acts as a high-pass filter and the reflected energy decreases even slower, proportional to $r^{-\epsilon}$, so that no squaring occurs.

Since the last report, a paper on the theoretical investigation of electromagnetic missiles at off-axis field points and their properties for the case when the launcher is a circular current disk has been published [6]. The results indicate that the electromagnetic-missile effect extends beyond the cylindrical region defined by the radius of the disk. Electromagnetic missiles are found to have the following

properties in addition to the slow decrease of energy: (1) The electromagnetic missile propagates with a waveform that remains similar in shape but diminishes in size. (2) The transverse distribution of energy around the axis is stable; when the longitudinal distance increases, the transverse pattern of the energy remains the same. This "plane-wave beam-like" property is different from continuous-wave (CW) radiation, in which the energy pattern is like that of a spherical wave. (3) The transverse energy pattern has a cusp on the axis. This property is also different from CW radiation. Although derived for the case of a current in a plane, these properties are also valid for other EM-missile launchers, such as the open-ended waveguide and the spherical lens.

The properties described above assume a uniform distribution of the electric field on the aperture. If the distribution of the current or the field is nonuniform, how are the properties of EM missiles, such as their waveforms, energy decay and transverse patterns affected? In another paper published during this period [7] the effects of a nonuniform distribution of the electric field on the aperture of a parabolic dish are examined. The general formulas for the EM field and associated energy radiated from a variety of nonuniformly distributed aperture fields are derived first with an unlimited spectrum and then with a limited spectrum, i.e., with a practically feasible excitation.

A study of a variety of continuous, nonuniform distributions in the aperture fields has found that: (1) The aperture field with a nonuniform distribution has the ability to launch an EM missile. (2) The effects of the nonuniform distribution are characterized by an angular average function. (3) The waveform of the radiated field excited by a single impulse consists of two mutually opposite pulses. For a fixed distance, its amplitude decreases with increasing nonuniformity of the source. (4) If the spectrum extends to infinity, the nonuniform distribution affects only the magnitude of the energy, not its rate of decay. (5) If the spectrum is limited, the

nonuniform distribution significantly affects the rate of decay of the energy. The more nonuniform the source, the faster the decay.

A second kind of nonuniform distribution, i.e., an array composed of point sources, has also been examined [7]. Strictly speaking, the energy radiated from such an array cannot decrease more slowly than $1/z^2$ since the decay parameter ϵ is constrained by the condition of finite total energy and, hence, must be greater than 1. However, for practical excitations where the frequency spectrum has a cutoff, the constraint that ϵ be greater than 1 does not necessarily apply. A numerical analysis has shown that, depending on the cutoff frequency, there is a minimum number of elements N and minimum distance z beyond which the energy from the array can decrease as slowly as the energy from a continuously distributed disk of the same size. The energy from a point-source array increases according to N^2 when the excitations are synchronous, but according to N when the excitations are random. If the elements of the array are "patch sources" rather than point sources, under certain conditions involving N and z, the energy radiated from the array can also achieve slow decay. Examples of patch sources include open waveguides, parabolic dishes, and lenses.

References:

1. T. T. Wu, "Electromagnetic Missiles," *J. Appl. Phys.* 57, 2370–2373 (1985).

2. J. M. Myers, T. T. Wu, and H. E. Brandt, "Electromagnetic Missiles from Currents on Fractal Sets," SPIE Proceedings, Vol. 1226, Intense Microwave and Particle Beams, 314–323 (1990).

3. H.-M. Shen, "Spherical Reflector as an Electromagnetic-Missile Launcher," *J. Appl. Phys.* 68, 1–7 (1990).

4. J. M. Myers, H.-M. Shen, T. T. Wu, and H. E. Brandt, "Curved Electromagnetic Missiles," SPIE Proceedings, Vol. 1061, Microwave and Particle Beam Sources and Directed Energy Concepts, 361–369 (1989).

5. J. M. Myers, and T. T. Wu, "Backscattering of Electromagnetic Missiles," SPIE Proceedings, Vol. 1226, Intense Microwave and Particle Beams, 290–301

(1990).

6. H.-M. Shen and T. T. Wu, "The Properties of the Electromagnetic Missile," *J. Appl. Phys.* 66, 4025–4034 (1989).

7. H.-M. Shen, "Electromagnetic Missile from a Nonuniform Aperture Field," SPIE Proceedings, Vol. 1226, Intense Microwave and Particle Beams, 278–289 (1990).

IV.8 Experimental Study of Electromagnetic Pulses with a Slow Rate of Decay. H.-M. Shen, R. W. P. King, and T. T. Wu, Grant N00014-89-J-1023, and Army LABCOM Contract DAAL02-89-K-0097; Research Unit 11.

The purpose of the experiment is to demonstrate missile-like electromagnetic pulses. More specifically, this is a program to build and test devices capable of launching electromagnetic missiles. The program must measure the EMP accurately enough to confirm the slow decay of the energy and provide the means for improving the design of the EM-missile launcher. Because a missile-like electromagnetic pulse (EMP) involves transients with rise times under 100 picoseconds, the measurement of short pulses is essential.

The experiment consists of an electromagnetic-missile launcher fed by a voltage pulse generator that radiates an EMP. The pulse travels above the ground plane, is received by an EMP sensor, and then recorded by a sampling oscilloscope. The platform is a 51 $\times$ 16 square-foot metal ground plane supported by a 4-foot-high wooden frame. The EM field is radiated, propagated, and received above the ground plane. Due to the image effect, the EM field above the ground plane is equivalent to that in free space.

In order to detect very short electromagnetic pulses under 100 picoseconds in width, a receiving antenna with a wide band from 0 to 14 GHz is needed. The usual short dipoles or monopoles do not provide both the required fidelity (bandwidth) and sensitivity. Two new EMP sensors—the L-antenna and the V-antenna—have been designed, analyzed and tested [1]. They are simple and inexpensive, and

can detect the electromagnetic pulse with both high fidelity and sensitivity. An approximate analysis is given in [1] for better understanding and optimum design of the proposed EMP antennas. Compared to other sensors of the same height, the bandwidth of the new sensors is two times wider; compared to sensors of the same bandwidth, the sensitivity is two times higher for the L-antenna and eight times higher for the V-antenna. Another advantage of the new sensors over the short dipoles is that there is no need for an integration to restore the waveform of the incident field; the output waveform is very nearly proportional to that of the incident field. This is a great advantage in the data processing since the integration would introduce significant error due to the DC offset. In the experimental study of electromagnetic missiles, the pulse widths detected by these new sensors is only 6% wider than that of the incident EMP.

In order to emit an EM pulse with a spherical wave front, a special feeding antenna—the V-conical antenna—has been designed, analyzed and tested [2]. Such a V-conical antenna has the ability to emit a pure spherical wave. This is very important in order to obtain an "in phase" plane-wave front at the aperture of the dish. Other advantages include the fact that its structure is suitable for combining with a lens or reflector, and a theoretical analysis of its properties is feasible.

After adopting the newly designed transmitting antenna (V-conical antenna) and receiving antenna (L-antenna), the entire system was found to work properly up to 10 GHz. In the first set of data reported two years ago [3], the measurements were taken at 16 evenly spaced observation holes along the z-axis on the ground plane. The EM pulse launcher was a parabolic dish. The measurements reported last year were taken of the off-axis electromagnetic fields launched from the parabolic dish on the ground plane. These results have now been published [4], [5]. The off-axis observation holes are located in the z direction at z = 13, 25, 37 and 49 feet. At each of these distances, there are five holes, with a 1-foot separation between them,

e.g., $x = 0, 1, \ldots, 4$ ft. The measured data show that: (1) The waveform of the EM field on the axis radiated from a parabolic dish excited by a single impulse consists of two mutually opposite pulses; when the off-axis distance x increases, the two pulses move apart and their amplitudes decrease; (2) the energy decreases transversely beyond the cylindrical region defined by the radius of the parabolic dish; and (3) the transverse distribution of the energy is stable within $z = 37$ feet; beyond this distance, the transverse distribution changes and spreads. An examination of the data indicates that the measured waveforms at different off-axis locations are comparable with those calculated from the theory. When the energy distributions are compared, however, the measured values appear to spread faster than their theoretical counterparts. This may be due to the mechanical error of the parabolic dish.

Measurements were then taken of the off-axis electric field from an open waveguide on the ground plane. The measured waveforms from the open waveguide are comparable to those measured from the parabolic dish, except for complications due to the presence of EM pulses reflected from the wall of the tube. The measurements show that the magnitude of the waveforms from the open waveguide has increased by only 6%, which is a smaller increase than predicted by the theory. This may be because the length of the waveguide is too short to establish a stable TE_{11} mode inside the tube.

Progress in the experimental investigation during the current year include the construction of a new hyperboloidal lens system consisting of a parabolic lens made of wax and a V-conical antenna with a 30° apex angle located at the focal point of the lens. The apparatus has been tested and adjusted and, as expected, the lens system performs like an aperture field, similar to that from a parabolic reflector. Both the measurement and simulation show that the electromagnetic missile launched from the hyperboloidal lens exhibits a similar slow rate of energy

decay and similar waveform consisting of a pair of opposite pulses. A paper on these results is being written [6].

References:

1. H.-M. Shen, R. W. P. King, and T. T. Wu, "New Sensors for Measuring Very Short Electromagnetic Pulses," *IEEE Trans. Antennas Propagat.* 38, 838–846 (1990).

2. H.-M. Shen, R. W. P. King, and T. T. Wu, "V-Conical Antenna," *IEEE Trans. Antennas Propagat.* AP-36, 1519–1525 (1988).

3. H.-M. Shen, "Experimental Study of Electromagnetic Missiles," SPIE Proceedings, Vol. 873, Microwave and Particle Beam Sources and Propagation, 338–346 (1988).

4. H.-M. Shen and T. T. Wu, "The Transverse Energy Pattern of an Electromagnetic Missile from a Circular Current Disk," SPIE Proceedings, Vol. 1061, Microwave and Particle Beam Sources and Directed Energy Concepts, 352–360 (1989).

5. H.-M. Shen and T. T. Wu, "The Properties of the Electromagnetic Missile," *J. Appl. Phys.* 66, 4025–4034 (1989).

6. H.-M. Shen, T. T. Wu and J. M. Myers, "Experimental Study of Electromagnetic Missiles from a Hyperboloidal Lens," to be presented at the SPIE OE/LASE'91 Conference on Intense Microwave and Particle Beams II, January 1991.

IV.9 Theoretical Studies of Circular Arrays of Dipoles. T. T. Wu, R. W. P. King, G. Fikioris, and B. H. Sandler, Grant N00014-89-J-1023, RADC Contract F19628-88-K-0024, and Army LABCOM Contract DAAL02-89-K-0097; Research Unit 11.

A review [1] of available data from numerous experimental and theoretical researches—many carried out over 25 years ago—combined with a very recent quantum-mechanical investigation [2], has led to new insights into the possibilities of closed loops of dipoles as highly directional arrays. The critical newly emphasized feature is the remarkable high-Q property of a correctly designed closed loop of coplanar dipoles when only one element is driven and all dimensions—the length of the elements, their cross-sectional size and shape, the number of elements, and

the circumference of the closed loop—are correctly chosen. Before investigating the potentially important applications of an egg-shaped array as a superdirective antenna, a systematic study of the properties of the circular array is necessary. In particular, improved methods for solving the integral equation for the current in a single element, i.e., the tubular antenna, are needed in order to analyze and design a resonant circular array more accurately. The results of these investigations are described below.

Because the two-term theory of circular arrays as formulated by Mack [3] has certain limitations, a more accurate formulation for the distribution of current on the elements has been derived. It is particularly essential with closely coupled long elements. The new work is contained in two papers by King [4], [5] that introduce a new approach to the analysis of arrays with elements that include some that are very closely spaced and many that are far apart. Of particular importance is the separation of elements into two groups, the one closely coupled with a strong effect on the distributions and amplitudes of the currents, the other with a far-field-like interaction.

In the first paper [4], the vector potential and electric field generated by the current in a center-driven or parasitic dipole antenna that extends from $z = -h$ to $z = h$ are investigated for each of the several components of the current. These include $\sin k(h - |z|)$, $\sin k|z| - \sin kh$, $\cos kz - \cos kh$, and $\cos \frac{1}{2}kz - \cos \frac{1}{2}kh$. Of special interest are the interactions among the variously spaced elements in parallel, nonstaggered arrays. These depend on the mutual vector potentials. It is shown that at a radial distance $\rho \sim h$ and in the range $-h \leq z \leq h$, the vector potentials due to all four components become alike and have an approximately plane-wave form. Simple approximate formulas for the electric fields and vector potentials generated by each of the four distributions are derived and compared with the exact results. The application of the new formulas to large arrays is discussed.

In the second paper [5], the circular array of parallel nonstaggered elements is investigated. It has unusual resonances when correctly proportioned. The analytical determination of its properties in their dependence on the radius, length, and spacing of the individual elements as well as on their number requires a high degree of accuracy. The solution of the coupled integral equations with the method of symmetrical components is reexamined with special attention to the problem of coupling among closely spaced and more distant elements. It is shown that the defining criterion for close coupling is not $kb_{ij} \leq 1$ but $b_{ij} \leq h$, where b_{ij} is the distance between elements i and j, h is their half-length and $k = 2\pi/\lambda$. This means that electrically short elements can be much closer together without close-coupling effects than long elements. The new study also shows that for electrically short elements the two-term approximation—which reduces to a shifted-cosine current in all parasitic elements—is an excellent approximation. The accuracy of the new general formula is verified for the four-element array and the single element.

An accurate analysis of the current near the open ends of a center-driven dipole has also been carried out [6], [7] as a necessary improvement on the trigonometric functions used to represent current distributions especially in long driven elements. An analysis of the current and charge distributions near the end of a tubular antenna using the Wiener-Hopf solution has shown that it is possible to derive accurate expressions for the current and charge near the end of a tubular antenna. The solution for the current near the end of the antenna is found to be a *universal* formula; i.e., when the frequency or length is changed, the relative distribution near the end remains the same. This is described in more detail under Topic IV.10.

References:

1. R. W. P. King, "Supergain Antennas and the Yagi and Circular Arrays," *IEEE Trans. Antennas Propagat.* AP-37, 178–186 (1989).

2. A. Grossmann and T. T. Wu, "A Class of Potentials with Extremely Narrow Resonances," *Chinese Jour. Phys.* 25, 129–139 (1987).

3. R. W. P. King, R. B. Mack, and S. S. Sandler, *Arrays of Cylindrical Dipoles*, Chapter IV, Cambridge Univ. Press (1968).

4. R. W. P. King, "Electric Fields and Vector Potentials of Thin Cylindrical Antennas," *IEEE Trans. Antennas Propagat.*, accepted for publication.

5. R. W. P. King, "The Large Circular Array with One Element Driven," *IEEE Trans. Antennas Propagat.*, accepted for publication.

6. H.-M. Shen and T. T. Wu, "The Universal Current Distribution Near the End of a Tubular Antenna," *J. Math. Phys.* 30, 2721–2729 (1989).

7. H.-M. Shen, R. W. P. King, and T. T. Wu, "The Combination of the Universal End-Current and the Three-Term Current on a Tubular Antenna," *J. Electromagn. Waves & Appl.* 4, 189–200 (1990).

IV.10 Asymptotic Solution for the Charge and Current Near the Open End of a Linear Tubular Antenna.

H.-M. Shen, T. T. Wu, and R. W. P. King, Grant N00014-89-J-1023, Army LABCOM Contract DAAL02-89-K-0097, and RADC Contract F19628-88-K-0024; Research Unit 11.

Since the dipole antenna is one of the most useful forms of antenna, it has been analyzed extensively for more than half a century. Most of these analyses have dealt with the case where the radius of the dipole is small. In such cases, since the vector potential on the surface of the dipole is roughly proportional to the current, its distribution obtained theoretically is approximately sinusoidal or, more generally, a sum of several sinusoidal terms. This traveling-wave-like solution is mainly caused by the aspect of electromagnetic induction. There is, however, another aspect of this problem of the current distributions on the dipole antenna. Coulomb repulsion between charges of the same sign is always present. This repulsion leads to a larger charge density near the end of the rod than at the center. For the dipole antenna, this Coulomb repulsion leads to the result that the charge density and, hence, also the current cannot be described naturally and accurately as a sum of sinusoidal terms. This effect is most pronounced near the ends of the antenna; it is the subject of a new paper [1].

The basic idea of the paper is to use the Wiener-Hopf procedure of solving integral equations. This is intimately related to the observation that, except possibly for an overall constant, the current distribution near one end of a dipole antenna is approximately independent of the details near the other end. First, the problem of the current distribution near the end of the center-driven dipole antenna, where Coulomb repulsion is most pronounced, is formulated in terms of a Wiener-Hopf integral equation, which is then solved exactly. This exact solution is then evaluated approximately using the fact that the radius of the dipole antenna is small. This last step is technically complicated. Much effort has been directed toward changing the contours of the integration to improve the convergence. It is found that the expression obtained for the current from the inverse Fourier transform is a *universal* formula in which no parameter other than the radius is involved; i.e., the relative distributions of charge and current are independent of the length of the antenna and the frequency of operation. This means that within the range of about a quarter-wavelength, the repulsion effect dominates the distributions of charge and current, so that these are significantly different from sinusoidal distributions which are the solutions from approximate theories.

With this newly derived universal formula for the current near the end of a tubular antenna, it is possible to improve the current distribution obtained previously [2] from the approximate three-term solution. In a second paper [3], the current near the end of the tube is represented by the universal formula derived in [1], the currents on the other parts of the antenna by the three-term solution. The currents and charges obtained from the two formulations are then matched at the junction. When the combined solution is compared with experimental results, it is seen that the currents at the end as well as the driving-point admittance have been improved significantly.

References:

1. H.-M. Shen and T. T. Wu, "The Universal Current Distribution Near the End of a Tubular Antenna," *J. Math. Phys.* 30, 2721–2729 (1989).

2. R. W. P. King and T. T. Wu, "Currents, Charges and Near Fields of Cylindrical Antennas," *J. Research NBS, Radio Science* 69D, 429–446 (1965).

3. H.-M. Shen, R. W. P. King, and T. T. Wu, "The Combination of the Universal End-Current and the Three-Term Current on a Tubular Antenna," *J. Electromagn. Waves & Appl.* 4, 189–200 (1990).

IV.11 **Properties of Closed Loops of Pseudodipoles.** T. T. Wu and D. K. Freeman, Grant N00014-89-J-1023, RADC Contract F19628-88-K-0024, and DOE Grant DE-FG02-84ER40158; Research Unit 11.

In order to obtain a general idea of how sensitively the behavior of a supergain antenna is related to its parameters, a circular array comprised of the simplest elements—point sources or pseudodipoles—is under investigation. The pseudodipole is a point interaction, i.e., the induced current density depends only on the value of the electric field at a point. It is therefore intuitively clear that if the pseudodipole is to approximate a physical dipole, the physical dipole should be, in some sense, small. Moreover, in order for such a small object to produce a significant scattered field, one expects that it must be resonant. This suggests the idea of taking a center-loaded cylindrical dipole, and letting its size tend to zero while simultaneously adjusting the load reactance in order to keep the magnitude of the scattered field constant. A paper is being written in which it is shown that, for an incident plane-wave, this procedure results in a scattered field which is precisely the scattered field of a pseudodipole. Although the calculation has been carried out for plane-wave scattering, the identification between pseudodipole and resonant cylindrical dipole is in fact more general. For example, the two-term theory can also be applied to a circular array of parallel, nonstaggered, resonant cylindrical dipoles, in which one element is driven and the rest are parasitic. In this case, the same identification is obtained. That this must be so becomes apparent in light of

recent investigations [1] which have shown that the vector potential impressed on one element of the array by another (for sufficiently large element separations) is essentially that of a plane wave, even when more sophisticated current approximations are used (see Topic IV.9). However, in what sense the identification between pseudodipole and resonant cylindrical dipole holds in general is not so clear.

Reference:

1. R. W. P. King, "Electric Fields and Vector Potentials of Thin Cylindrical Antennas," *IEEE Trans. Antennas Propagat.*, accepted for publication.

IV.12 Closed Loops of Parallel Coplanar Dipoles—Electrically Short Elements. T. T. Wu, R. W. P. King, and G. Fikioris, Grant N00014-89-J-1023, Army LABCOM Contract DAAL02-89-K-0097, and RADC Contract F19628-88-K-0024; Research Unit 11.

The first attempt to extend the analysis of large circular arrays to short lengths—specifically to the length $2h/\lambda = 0.36$ predicted for minimum loss [1, Fig. 5]—was not successful; no sharp resonances occurred. When the thickness of the elements was later increased from $a/\lambda = 0.007022$ to $a/\lambda = 0.028$, the results were startlingly different. The thicker array displays a remarkable set of sharp resonances. Investigation shows that each resonance corresponds to a particular dominant phase-sequence conductance $G^{(m)}$ in the sum over the $N/2$ phase sequences that determine the $N/2$ different currents. A study of the self- and mutual admittances (normalized currents) and far-field patterns of some of the phase sequences in arrays of 60, 72 and 90 elements has disclosed a remarkable set of properties [2]. Use is made of the method of symmetrical components and a two-term representation of current in each element. The arrays studied have only one driven element. The results—which are displayed in a sequence of graphs—indicate that the relative currents in the elements can be distributed in triplets, triplets alternating with singlets, two independent sets of singlets, or one set of singlets. These are described

in turn below.

The $m = 10$ resonance with $N = 60$ is particularly interesting. The currents in the 60 elements form 20 *triplets* or groups of three, viz., 3-4-5, 6-7-8, ..., 60-1-2. The currents in the three elements in each group are almost in phase; the phase difference between the central elements in adjacent triplets is exactly 180°. The magnitude of the current in each central element is about double that in the adjacent two and very nearly equal to that in the central elements of the other triplets. The single exception is the driven element #1 which carries a current twice as large. The far-field power pattern consists of 20 sharp peaks between 20 nulls. The peaks occur in the directions of the central elements 1, 4, 7, ..., of the 20 triplets. The larger current in the driven element and the lack of exact equality in the phases of the currents in each triplet represent a rotational asymmetry with more power radiated in the backward direction.

For the $m = 9$ resonance with $N = 72$, the magnitudes and phases of the normalized currents in the elements are separated into 18 groups of triplets (4-5-6, 8-9-10, 12-13-14, ..., 72-1-2) with large currents and 18 singlets (3, 7, 11, ..., 71) with very small currents. The central elements of the triplets have the largest and almost equal currents. They differ in phase from one group of three to the next group of three by 180°. However, these groups of three are not adjacent but separated by the singlets. These have small currents and phases that differ by exactly 90° from the central elements of the adjacent triplets. The 18 peaks in the field pattern are determined by the 18 triplets. The deep minima (nulls) lie along the directions of the singlets which contribute little to the field.

For the $m = 18$ resonance for $N = 72$, the magnitudes and phases of the normalized currents are clearly divided between two groups of 36 elements, the odd-numbered elements (1, 3, ..., 71) with large currents and the even-numbered elements (2, 4, ..., 72) with small currents. The phase difference from element to

element within each group is 180°; from element to adjacent element it is 90°. Thus, each group is in the approximately neutral plane of the other. The field pattern has 36 peaks in the directions of the odd elements and 36 minima in the directions of the even elements.

In order to generate singlets, it is necessary that $m = N/2$. With $N = 90$, $m = 45$, the associated resonance peak is extremely sharp. It occurs at $d/\lambda = 0.437432095$ and the self-conductance $G_{1,1}$ has the very large value 3.256 Amp/V. The self- and mutual conductances of all of the elements alternate between equal and very large positive and negative values. The associated susceptances are very small compared to the conductances, and the self-susceptance $B_{1,1}$ of the driven element #1 is very close to zero. This means that the driving-point impedance of the entire array at the terminals of element #1 *is a pure resistance* near 0.3 Ohm. The magnitudes of the normalized currents range from 3.255 Amp for the driven element to 3.235 Amp in element 45. The associated phases are alternately 0° and 180°. The far-field power pattern consists of 90 nulls between 90 very sharp spikes.

This most recent work on this problem has been motivated by studies of the pseudopotential and the pseudodipole. A new more accurate imaginary part of the phase-sequence kernel for the circular array of dipoles has been found; it consists of a double integral. When expanded in powers of ka, the leading term in the expansion of the imaginary part is $[\sin k(z - z')]/k(z - z')$, which is precisely the imaginary part of the self-term of the kernel used up until now but with ka set to zero. This simple change results in greater accuracy. This is expected to be true as well for the self-term in the integral equations of an array of arbitrary shape (see Topic IV.13). The change has significant consequences. When $d/\lambda < m/N$, the new imaginary part $K_I^{(m)}(z)$ is exponentially small in N. As a result, $K_I^{(m)}(z)$ will be evaluated either directly using quadruple precision or by an asymptotic formula valid for large N.

References:

1. R. W. P. King, "Supergain Antennas and the Yagi and Circular Arrays," *IEEE Trans. Antennas Propagat.* AP-37, 178–186 (1989).

2. G. Fikioris, R. W. P. King, and T. T. Wu, "The Resonant Circular Array of Electrically Short Elements," *J. Appl. Phys.*, accepted for publication.

IV.13 Closed Loops of Parallel Coplanar Dipoles—Arrays of Arbitrary Shape. T. T. Wu, R. W. P. King, and G. Fikioris, Grant N00014-89-J-1023, Army LABCOM Contract DAAL02-89-K-0097, and RADC Contract F19628-88-K-0024; Research Unit 11.

The two-term theory for an array of parallel, nonstaggered dipoles has been generalized from a circular array to one of arbitrary shape. The generalized theory makes the same approximations used for the circular array, but does not employ the method of symmetrical components for which circular symmetry is necessary. It is shown analytically that, in the special case of a circular array, the two theories give identical results. The new theory has been used to study the properties of "egg-shaped" arrays. An equation describing an egg shape, i.e., an analytic closed curve that is not symmetric with respect to the x-axis, is obtained by adding a term proportional to x^3 to the equation of an ellipse. The variation of the three parameters in this equation provides a wide variety of egg shapes. Far fields and current amplitudes in the elements around the array have been obtained for several different egg shapes with the parameters all the same as for the $N = 60$ triplets case in the circular array. It is seen that the current distribution around the array—in both amplitude and relative phase—is almost identical to that for the corresponding circular array. The field pattern is also similar; it consists of 20 peaks, the sharpness of which depends on the shape of the curve. None of the field distributions obtained was very different, however, from that for the circular array. The field pattern does change for an ellipse of very large eccentricity; as expected, it is of the endfire type and very similar to that of a 30-element Yagi array.

IV.14 Plasma Waveguide: A Concept to Transfer EM Energy in Space.

H.-M. Shen, Grant N00014-89-J-1023 and Army LABCOM Contract DAAL02-89-K-0097; Research Unit 11.

It is known that, when an ultraviolet laser beam passes through a low-pressure gas background, along its path the laser beam will photo-ionize the atoms of the gas and create a partially ionized channel. A plasma channel of this type has been used successfully to suppress the beam-breakup instability in the advanced accelerator; in the experiment a plasma column was created over a distance of up to 95 m [1]. It has also been suggested as a guiding mechanism for charged particle beams for use in the tenuous upper atmosphere of the earth [2]. Depending on the energy of the laser beam, a plasma channel ranging up to hundreds of kilometers can be generated.

The question arises, can such a plasma channel be used to guide electromagnetic (EM) waves? Is it a dielectric waveguide like an optical fiber? A dielectric waveguide is constructed of two media, the inside core and the outside cladding. The EM waves are confined by the total internal reflection between the two media. Thus, the index of refraction of the inside core must be larger than that of the outside cladding. Since the permittivity of the plasma is always smaller than that of the neutral gas, the solid plasma channel is not a guided EM-wave system. In order to confine the EM wave, the waveguide should be built with the vacuum (or neutral gas) core inside and a concentric plasma cladding outside. Such a structure is similar to the traditional dielectric waveguide except that the permittivity of the cladding of the plasma waveguide is strongly frequency-dependent.

Recently, the possibility of using a laser-generated "plasma waveguide" to transfer electromagnetic (EM) energy has been examined [3], [4]. The plasma waveguide is a cylindrical vacuum core surrounded by a plasma cladding. The analysis shows that guided-mode fields do exist inside the core. Like a general dielectric

waveguide, the plasma waveguide is characterized by a "normalized frequency parameter" (also called the V-number). Although the permittivity of the plasma varies strongly with frequency, the V-number surprisingly remains constant over the entire frequency range. Because of this property, the frequency dependence of the plasma waveguide is different; it has a wider high-frequency response than the general dielectric waveguide. The EM pulse can propagate in the plasma waveguide at close to the speed of light and keep its profile and shape unchanged. When the V-number is smaller than 2.4048 (the first root of the zero-order Bessel function), only the single HE_{11}-mode exists in the plasma waveguide. Unlike the dielectric waveguide, however, there is no high-frequency limitation for single-mode propagation. The EM fields outside the core in the plasma decrease exponentially with increasing radius. Thus, practically, a plasma cladding of sufficient thickness is all that is required to confine the EM wave. Such a plasma waveguide can be generated by a hollow laser beam in upper space and used for guiding EM pulses. A brief survey on laser-generated plasmas is given.

References:

1. D. S. Prono, "Recent Progress of the Advanced Test Accelerator," *IEEE Trans. Nucl. Sci.* NS-32, 3144–3148 (1985).

2. APS Study Group, "APS Study: Science and Technology of Directed Energy Weapons," *Rev. Mod. Phys.* 59, No. 3, Part II, Sec. 4.2, S71–S79 (1987).

3. H.-M. Shen, "Plasma Waveguide," SPIE Proceedings, Vol. 1226, Intense Microwave and Particle Beams, 302–313 (1990).

4. H.-M. Shen, "Plasma Waveguide: A Concept to Transfer EM Energy in Space," *IEEE Trans. Microwave Theory & Tech.*, submitted for publication.

ANNUAL REPORT OF

PUBLICATIONS/PATENTS/PRESENTATIONS/HONORS

a. Papers Submitted to Refereed Journals (and not yet published)

R. W. P. King, "On the Radiation Efficiency and the Electromagnetic Field of a Vertical Electric Dipole in the Air Above a Dielectric or Conducting Half-Space," *J. Electromagn. Waves & Appl.* (accepted).

R. W. P. King, "Electric Fields and Vector Potentials of Thin Cylindrical Antennas," *IEEE Trans. Antennas Propagat.* (accepted). (Partial support from RADC Contract F19628-88-K-0024 and Army LABCOM Contract DAAL02-89-K-0097.)

R. W. P. King, "The Large Circular Array with One Element Driven," *IEEE Trans. Antennas Propagat.* (accepted). (Partial support from RADC Contract F19628-88-K-0024 and Army LABCOM Contract DAAL02-89-K-0097.)

G. Fikioris, R. W. P. King, and T. T. Wu, "The Resonant Circular Array of Electrically Short Elements," *J. Appl. Phys.* (accepted). (Partial support from RADC Contract F19628-88-K-0024 and Army LABCOM Contract DAAL02-89-K-0097.)

H.-M. Shen, "Plasma Waveguide: A Concept to Transfer EM Energy in Space," *IEEE Trans. Microwave Theory & Tech.* (Partial support from Army LABCOM Contract DAAL02-89-K-0097.)

b. Papers Published in Refereed Journals

R. W. P. King, "Lateral Electromagnetic Pulses Generated on a Plane Boundary Between Dielectrics by Vertical and Horizontal Dipole Sources with Gaussian Pulse Excitation," *J. Electromagn. Waves & Appl.* 3, 589–597 (1989).

R. W. P. King, "Lateral Electromagnetic Waves from a Horizontal Antenna for Remote Sensing in the Ocean," *IEEE Trans. Antennas Propagat.* AP-37, 1250–1255 (1989).

R. W. P. King, "Electromagnetic Field of a Vertical Dipole Over an Imperfectly Conducting Half-Space," *Radio Science* 25, 149–160 (1990).

R. W. P. King, "Lateral Electromagnetic Waves and Pulses on Open Microstrip," *IEEE Trans. Microwave Theory & Tech.* 38, 38–47 (1990).

H.-M. Shen and T. T. Wu, "The Properties of the Electromagnetic Missile," *J. Appl. Phys.* 66, 4025–4034 (1989). (Partial support from Army LABCOM Contract DAAL02-89-K-0097.)

H.-M. Shen and T. T. Wu, "The Universal Current Distribution Near the End of a Tubular Antenna," *J. Math. Phys.* 30, 2721–2729 (1989). (Partial support from Army LABCOM Contract DAAL02-89-K-0097 and RADC Contract F19628-88-K-0024.)

H.-M. Shen, R. W. P. King, and T. T. Wu, "The Combination of the Universal End-Current and the Three-Term Current on a Tubular Antenna," *J. Electromagn. Waves & Appl.* 4, 189–200 (1990). (Partial support from Army LABCOM Contract DAAL02-89-K-0097 and RADC Contract F19628-88-K-0024.)

H.-M. Shen, R. W. P. King, and T. T. Wu, "New Sensors for Measuring Very Short Electromagnetic Pulses," *IEEE Trans. Antennas Propagat.* 38, 838–846 (1990). (Partial support from Army LABCOM Contract DAAL02-89-K-0097.)

H.-M. Shen, "Spherical Reflector as an Electromagnetic-Missile Launcher," *J. Appl. Phys.* 68, 1–7 (1990). (Partial support from Army LABCOM Contract DAAL02-89-K-0097.)

h. Contributed Presentations at Topical or Scientific/Technical Society Conferences

H.-M. Shen and T. T. Wu, "The Transverse Energy Pattern of an Electromagnetic Missile from a Circular Current Disk," SPIE Proceedings, Vol. 1061, Microwave and Particle Beam Sources and Directed Energy Concepts, 352–360 (1989). (Partial support from Army LABCOM Contract DAAL02-86-K-0095.)

J. M. Myers, H.-M. Shen, T. T. Wu, and H. E. Brandt, "Curved Electromagnetic Missiles," SPIE Proceedings, Vol. 1061, Microwave and Particle Beam Sources and Directed Energy Concepts, 361–369 (1989). (Partial support from Army LABCOM Contract DAAL02-86-K-0095.)

T. T. Wu, H.-M. Shen, and J. M. Myers, "A Review of Electromagnetic Missiles," SPIE Proceedings, Vol. 1061, Microwave and Particle Beam Sources and Directed Energy Concepts, 370–379 (1989). (Partial support from Army LABCOM Contract DAAL02-86-K-0095.)

H.-M. Shen, "Electromagnetic Missile from a Nonuniform Aperture Field," SPIE Proceedings, Vol. 1226, Intense Microwave and Particle Beams, 278–289 (1990). (Partial support from Army LABCOM Contract DAAL02-89-K-0097.)

J. M. Myers, and T. T. Wu, "Backscattering of Electromagnetic Missiles,"

SPIE Proceedings, Vol. 1226, Intense Microwave and Particle Beams, 290–301 (1990). (Partial support from Army LABCOM Contract DAAL02-89-K-0097.)

H.-M. Shen, "Plasma Waveguide," SPIE Proceedings, Vol. 1226, Intense Microwave and Particle Beams, 302–313 (1990). (Partial support from Army LABCOM Contract DAAL02-89-K-0097.)

J. M. Myers, T. T. Wu, and H. E. Brandt, "Electromagnetic Missiles from Currents on Fractal Sets," SPIE Proceedings, Vol. 1226, Intense Microwave and Particle Beams, 314–323 (1990). (Partial support from Army LABCOM Contract DAAL02-89-K-0097.)

j. Graduate Students and Post-Doctorals Supported under the JSEP for the Year Ending 30 June 1990

Dr. J. M. Myers, Dr. H.-M. Shen, Mr. G. Fikioris, Mr. D. K. Freeman.

V. SIGNIFICANT ACCOMPLISHMENTS REPORT

V.1 Second-harmonic Efficiency and Reflectivity of GaAs During Femtosecond Melting.

N. Bloembergen, E. Mazur, P. Saeta, Y. Siegal and J. K. Wang; Research Unit 7, QUANTUM ELECTRONICS.

Studies of the ultrafast melting of semiconductor surfaces under intense laser irradiation at frequencies above the bandgap reveal changes in the dielectric properties on the sub-picosecond timescale. Reflectivity measurements of silicon with femtosecond pulses demonstrate significant changes within 300 fs [1]. Second-harmonic measurements on silicon further show that the top 70–130 Å of the silicon surface loses its cubic symmetry within 150 fs [1]. In this paper we report on simultaneous reflectivity and second-harmonic generation (SHG) measurements during the melting of GaAs with 160-fs laser pulses. The results show bulk melting to a depth of at least 90 atomic layers within the pulsewidth.

Amplified 200-μJ pulses at 620 nm are split into a pump and a probe beam with an energy ratio of 20:1. The p-polarized probe pulse is incident upon a (100) GaAs surface at 45°; the pump is orthogonally polarized and enters along the normal. The probe interrogates the central one-tenth of the pumped area. We determine the origin of time by attenuating the pump beam and maximizing the reflection sum frequency signal of the pump and probe beams. For each laser shot, the reflected intensity and the second-harmonic intensity are measured. In addition, we check for the presence of broadband ultraviolet radiation from a surface plasma. The pump beam by itself generates no spurious reflection or second-harmonic signal.

Figure 1 summarizes the reflectivity measurements normalized to the appropriate value for negative times. The dip in reflectivity at low fluence in the temporal range of — 130 fs to +1.9 ps can be attributed to a dense free-carrier plasma cre-

ated by photoexcitation [2]. This plasma decreases the real part of the dielectric constant, leading to a drop in reflectivity. By +130 fs the reflectivity at high fluence rises to roughly twice the crystalline value, consistent with the value predicted by a Drude model for metallic molten GaAs. After 50 ps the reflectivity at high fluence drops dramatically. This drop is probably due either to heating of the molten material far above the melting temperature [3], or to the delayed formation of a plasma cloud in front of the surface [4,5].

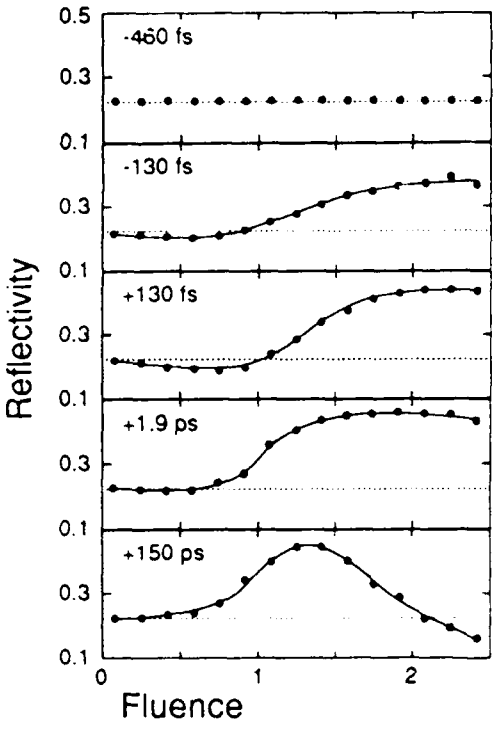

Figure V.1 GaAs reflectivity vs. fluence for various time delays. F_0 is the minimum fluence at which the SH efficiency drops to zero.

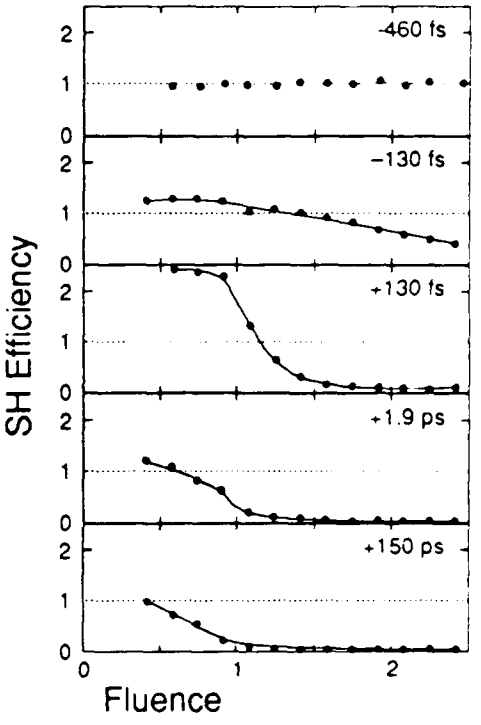

Figure V.2 GaAs second-harmonic efficiency vs. fluence for various time delays. F_0 is the minimum fluence at which the SH efficiency drops to zero.

The second-harmonic signal is divided by the square of the probe intensity to obtain the second-harmonic (SH) efficiency, normalized to unity for unpumped material. Figure 2 shows a rapid, dramatic decrease to zero in SH efficiency as early as +130 fs, coincident with the observed plateau in reflectivity. The absence of any

second-harmonic signal in this region indicates melting to a depth of at least 90 atomic layers, the absorption depth of the second harmonic.

Concurrent with the observed dip in reflectivity at short times and low fluence one finds a marked increase in SH efficiency. This increase is caused by a change in index of refraction due to the presence of the free-carrier plasma. First, lowered reflectivity results in an increased probe intensity beneath the surface. Second, with a decrease in the real part of the index, the angle between the probe E-field inside the material and the $\langle 0\bar{1}0 \rangle$ crystal axis increases from 10° to about 15°, resulting in approximately a factor 2 increase in SH efficiency.

We also measured the reflectivity and SH efficiency after complete equilibration of the material. The reflectivity rises again and settles at a value of 0.24, slightly higher than the value of crystalline GaAs (0.22), but lower than that of amorphous GaAs (0.28); the SH efficiency recovers to roughly half its original value. The net increase in reflectivity rules out any ablation of surface material, while the second harmonic from the resolidified material suggests a partial recrystallization.

In summary, we have performed femtosecond pump-probe measurements of the second-harmonic efficiency and reflectivity of GaAs during melting. Within 200 fs the second-harmonic signal drops to zero at high fluence, indicating melting to a depth of at least 90 atomic layers.

References:

1. H. W. K. Tom, G. D. Aumiller, and C.H. Brito-Cruz, *Phys. Rev. Lett.*60, 1438 (1988).
2. C. V. Shank, R. Yen, and C. Hirlimann, *Phys. Rev. Lett.*50, 454 (1983).
3. M. C. Downer, R. L. Fork, and C. V. Shank, *J. Opt. Soc. Am.*B2, 595 (1985).
4. J. M. Liu, A. M. Malvezzi, and N. Bloembergen, *Appl. Phys. Lett.*49, 622 (1986).

V.2 Electromagnetic Field of a Vertical Dipole over Earth or Sea with Applications to Communications and Over-the-Horizon Radar.

R. W. P. King and T. T. Wu; Research Unit 11, ELECTROMAGNETIC PHENOMENA.

In a series of papers beginning in 1909, Sommerfeld [1]–[3] derived exact, highly complex integrals for the Hertz potential of an infinitesimal vertical electric dipole over the earth or sea. Since then, attempts have been made by many investigators—including especially Norton [4], [5] and Baños [6]—to obtain useful explicit formulas for the associated electromagnetic field. However, even the most general, relatively simple formulas of King [7] imposed the restriction that the radial distance from the source to the receiver be large compared to both the height of the dipole and the height of the point of observation over the surface of the earth or sea. A major new analytical procedure by Wu and contained in a new paper by King [8] removes this restriction and has for the first time led to new, completely general, simple formulas for the electromagnetic field at any point—near or far, high or low—of a vertical dipole at any height over the earth or sea. The very simple far-field formula for the dipole on the surface consists of a space-wave term—representing the plane-wave reflection coefficient—which vanishes everywhere on the earth's surface and a surface-wave term that has its maximum along the surface of the earth and decreases rapidly away from the surface. A significant fact disclosed by the new formula is that the space wave as well as the surface wave decrease with radial distance as $1/r^2$ near the earth's surface where z/r is small. Communication between vertical antennas on the earth depends entirely on the surface wave. Over-the-horizon radar makes use of the space wave with ionospheric reflection and the surface wave for direct reflection from a low-flying missile or aircraft. The availability of unrestricted formulas for the complete electromagnetic field of vertical dipoles over earth or sea with arbitrary dielectric and conducting properties provides a new tool for accurate design and complete physical understanding.

References:

1. A. Sommerfeld, "Propagation of Waves in Wireless Telegraphy," *Ann. d. Phys.* 28, 665–736 (1909).

2. A. Sommerfeld, "Propagation of Waves in Wireless Telegraphy," *Ann. d. Phys.* 81, 1135–1153 (1926).

3. A. Sommerfeld, in *Die Differential u. Integralgleichungen der Mechanik u. Physik*, Vol. II, Ch. 23, P. Frank and R. v. Mises, Eds., F. Vieweg and Son, Braunschweig, Germany (1935).

4. K. A. Norton, "The Propagation of Radio Waves Over the Surface of the Earth and in the Upper Atmosphere," *Proc. IRE* 24, 1367–1387 (1936).

5. K. A. Norton, "The Calculations of Ground-Wave Field Intensity Over a Finitely Conducting Spherical Earth," *Proc. IRE* 29, 623–639 (1941).

6. A. Baños, Jr., *Dipole Radiation in the Presence of a Conducting Half-Space*, Pergamon Press, Oxford, England (1966).

7. R. W. P. King, "New Formulas for the Electromagnetic Field of a Vertical Electric Dipole in a Dielectric or Conducting Half-Space Near its Horizontal Interface," *J. Appl. Phys.* 53, 8476–8482 (1982); Erratum, 56, 3366 (1984).

8. R. W. P. King, "Electromagnetic Field of a Vertical Dipole Over an Imperfectly Conducting Half-Space," *Radio Science* 25, 149–160 (1990).